OXFORD GENETICS

GENETICS, 2023, 225(1), iyad118
https://doi.org/10.1093/genetics/iyad118
Advance Access Publication Date: 26 June 2023
Investigation

In vivo characterization of the maturation steps of a pigment dispersing factor neuropeptide precursor in the *Drosophila* circadian pacemaker neurons

Gyunghee G. Lee,[1] Kevin Zeng,[1] Cole M. Duffy,[1] Yadali Sriharsha,[1] Siuk Yoo,[2] Jae H. Park[1,3,4,*]

[1]Department of Biochemistry & Cellular and Molecular Biology, University of Tennessee, Knoxville, TN 37996, USA
[2]Department of Life Sciences, Yeungnam University, Gyeongsan, Gyeongbuk 38541, Korea
[3]Genome Science and Technology Graduate Program, University of Tennessee, Knoxville, TN 37996, USA
[4]NeuroNET Research Center, University of Tennessee, Knoxville, TN 37996, USA

*Corresponding author: Department of Biochemistry & Cellular and Molecular Biology, University of Tennessee, 1311 Cumberland Ave., Knoxville, TN 37996, USA. Email: jhpark@utk.edu

Abstract

Pigment dispersing factor (PDF) is a key signaling molecule coordinating the neuronal network associated with the circadian rhythms in *Drosophila*. The precursor (proPDF) of the mature PDF (mPDF) consists of 2 motifs, a larger PDF-associated peptide (PAP) and PDF. Through cleavage and amidation, the proPDF is predicted to produce cleaved-PAP (cPAP) and mPDF. To delve into the in vivo mechanisms underlying proPDF maturation, we generated various mutations that eliminate putative processing sites and then analyzed the effect of each mutation on the production of cPAP and mPDF by 4 different antibodies in both ectopic and endogenous conditions. We also assessed the knockdown effects of processing enzymes on the proPDF maturation. At the functional level, circadian phenotypes were measured for all mutants and knockdown lines. As results, we confirm the roles of key enzymes and their target residues: Amontillado (Amon) for the cleavage at the consensus dibasic KR site, Silver (Svr) for the removal of C-terminal basic residues from the intermediates, PAP-KR and PDF-GK, derived from proPDF, and PHM (peptidylglycine-α-hydroxylating monooxygenase) for the amidation of PDF. Our results suggest that the C-terminal amidation occurs independently of proPDF cleavage. Moreover, the PAP domain is important for the proPDF trafficking into the secretory vesicles and a close association between cPAP and mPDF following cleavage seems required for their stability within the vesicles. These studies highlight the biological significance of individual processing steps and the roles of the PAP for the stability and function of mPDF which is essential for the circadian clockworks.

Keywords: prohormone maturation, amidation, neuropeptide, circadian rhythms

Introduction

Circadian rhythms are various kinds of biological rhythms with approximately (circa) 24-h periodicity and are essential for the adaptation of most life forms on Earth. In animals, the circadian rhythms are governed by self-sustaining pacemaker cells in the brain. These cells synchronize their internal clock with environmental time cues (Zeitgeber) and autonomously maintain it in the absence of the Zeitgeber. The self-ticking central clockworks produce output signals to regulate diverse physiological and behavioral rhythms.

The site of the pacemaker cells in the mammalian brain is the hypothalamic suprachiasmatic nucleus (SCN) located just above the optic chiasm (Welsh *et al.* 2010). Extensive studies have shown that the autonomous molecular clock operating in the SCN is driven by autoregulatory transcriptional/translational feedback loops of major clock genes, *Clock*, *Bmal*, *Period genes* (*Per1-3*), and *Cryptochrome genes* (*Cry1* and 2) (Welsh *et al.* 2010). In addition, synchronization or coupling of a heterogeneous population of ~20,000 cells in the SCN is mediated primarily by a neuropeptide vasoactive intestinal peptide (VIP) and minorly by gastrin-releasing peptide (GRP), arginine vasopressin (AVP), and GABA (Vosko *et al.* 2007; Welsh *et al.* 2010; Ono *et al.* 2021).

Fundamental aspects of the clock-ticking mechanisms are well conserved in the vinegar flies, *Drosophila melanogaster*. Like those in mammals, transcriptional–translational feedback mechanisms of the core transcription factors, *period* (*per*), *timeless* (*tim*), *Clock* (*Clk*), and *cycle* (*cyc*, a homolog of mammalian *Bmal*), are essential for the generation of the autonomous clock (Hardin and Panda 2013). Comprehensive transgenic and histological investigations identified about 150 neurons expressing the core clock genes in an adult fly brain, suggesting them to be neuronal regulators of the circadian rhythms. Among them, a set of ventrally located lateral neurons (LN_vs) expressing the pigment dispersing factor (PDF) has been demonstrated as the essential pacemaker for circadian behaviors (Helfrich-Forster 2005). Furthermore, a null mutation of the *Pdf* gene and ablation of the PDFergic neurons display similarly abnormal circadian phenotypes, suggesting PDF to be a key circadian clock messenger from the pacemaker neurons (Renn *et al.* 1999).

Received: May 19, 2023. **Accepted:** June 13, 2023

In an adult brain, the PDF-expressing LN_v neurons are further resolved into 2 clusters, each containing 4 neurons referred to as small-LN_vs (s-LN_vs) and large-LN_vs (l-LN_vs), based on their distinct neuroanatomical features (Helfrich-Forster 2003, 2005). Several genetic and histological studies have confirmed that the s-LN_vs are particularly critical for entraining and maintaining the circadian locomotor activity rhythms (Renn *et al.* 1999; Yang and Sehgal 2001; Shafer and Taghert 2009). Interestingly, the PDF receptor (PDFR) is expressed in the s-LN_vs and several other clock-relevant neuronal clusters, suggesting that autocrine and paracrine actions of the PDF signaling establish intercellular communication among various subsets of clock gene-expressing neurons, which is necessary for entrainment, enforcement, and maintenance of the circadian pace-making system (Shafer *et al.* 2008; Im and Taghert 2010; Choi *et al.* 2012; Ahmad *et al.* 2021). In this aspect, PDF is considered a functional homolog of the mammalian neuropeptides produced in the SCN (Vosko *et al.* 2007).

Despite the importance of PDF as an essential clock-output component, little is known about how PDF production is regulated. *Pdf* transcript levels do not show daily oscillation but *Pdf* transcription is positively regulated by 2 major clock genes, *Clk* and *cyc*, particularly in the s-LN_v neurons through a yet unknown mechanism (Park and Hall 1998; Blau and Young 1999; Park *et al.* 2000; Park 2002; Bahn *et al.* 2009). On the contrary, *Clk* was shown to suppress *Pdf* expression perhaps indirectly via activation of *dhr38* and *stripe* in the s-LN_vs (Mezan *et al.* 2016). PDF levels are also regulated at the posttranscriptional level. At nerve terminals derived from the s-LN_vs, PDF immunoreactivities show circadian rhythms and such rhythms are under the control of *per* and *tim* (Park *et al.* 2000). Recent studies have shown that VRILLE, a transcription factor regulated by *Clk* and *cyc*, is also involved in the posttranscriptional regulation of PDF production in the s-LN_vs (Blau and Young 1999; Gunawardhana and Hardin 2017). Together, these studies indicate that PDF production is regulated at both the transcriptional and posttranscriptional levels. However, the molecular mechanisms underlying PDF production are only slightly understood.

Like the majority of other neuropeptides, the mature PDF (mPDF) is part of a much larger precursor form. *Drosophila Pdf* mRNA encodes a 102-amino-acid (aa)–long preproPDF, which consists of an N-terminal signal peptide, PDF-associated peptide (PAP), and PDF (Park and Hall 1998; Bahn *et al.* 2009). Following removal of the signal peptide, the remaining precursor form (proPDF) is expected to be cleaved at consensus dibasic Lys-Arg residues (-KR↓-) by a specific endopeptidase called prohormone convertase (for short, PC; Duckert *et al.* 2004; Hoshino and Lindberg 2012). The resulting products, PAP-KR and PDF-GK, undergo further modifications; removal of the C-terminal basic residues by a carboxypeptidase generates cleaved-PAP (cPAP) and PDF-G. The latter is then C-terminally amidated (PDF-NH_2) (Eipper *et al.* 1992, 1993; Pauls *et al.* 2014). In this study, we attempted to gain insights into the in vivo mechanisms underlying individual processing steps of proPDF and to assess the biological significance of each step and the roles played by the PAP domain.

Materials and methods

Drosophila stocks

The following driver and mutant lines were used in this study: *Pdf-Gal4* (Park *et al.* 2000), *DvPdf-Gal4* (Bahn *et al.* 2009), *Crz-Gal4* (Choi *et al.* 2006, 2008), *Akh-Gal4* (Lee and Park 2004), *ccap-Gal4* (Park *et al.* 2003), *386Y-Gal4* (Taghert *et al.* 2001), *c929-Gal4* (Hewes *et al.* 2003), and Pdf^{01} (Renn *et al.* 1999). Canton-S and w^{1118} were used as wild-type and genetic control, respectively. The TRiP or RNAi lines obtained from the Bloomington Drosophila Stock Center (BDSC) were used to knockdown genes encoding enzymes that are known for processing and amidation of *Drosophila* neuropeptides: UAS-amon-RNAi (BDSC #29009), GL01217(BDSC #41635), HM05071 (BDSC #28583), and HMS02715 (BDSC #44001) for *amon*; HMC04080 (BDSC #55392) for *PHM*, and HMC02395 (BDSC #44487) for *silver* (*svr*).

Site-directed mutagenesis

Fifteen Canton-S flies were homogenized in 500 μL of squash buffer (10 mM Tris, PH 8.0; 25 mM NaCl; 1 mM EDTA) containing 200 μg/mL proteinase K (Promega), incubated at 37°C for 25–30 min, and then at 95°C for 5 min to inactivate the proteinase K. Following centrifugation at max for 1 min, 1-μL aliquot of the supernatant was added to a 50-μL PCR using Easy-A High-Fidelity PCR Mastermix (Agilent) to amplify the genomic *Pdf* sequence (−770 to +1,127 relative to the transcription start site). PCR primers used for this reaction are PDF-Nsi-for and PDF-BH-rev primers (Table 1). The PCR product was purified by Qiaquick purification kit (Qiagen) and then cloned into pGEMTeasy vector (Promega). The recombinant DNA clone without PCR error was amplified and used as a template for the site-directed mutagenesis.

To eliminate putative PC-target sites (K81-R82), K81-codon was changed to Gln-codon (K81Q; Anstrom *et al.* 2006) by using Q5 site-directed mutagenesis kit (NEB), *Pdf* genomic DNA template, and K81Q-f and K81-r primers (Table 1), according to the manufacturer's protocol. To produce cPAP only from the proPDF, K81-codon was replaced with a stop codon (K81X) by using K81X-f and K81-r primers. To prevent potential stop codon read-through (Jungreis *et al.* 2011; Chen *et al.* 2020), double-stop codons were introduced to the K81X-f primer. To determine the importance of the C-terminal amidation of PDF, 3 different mutations were generated: G101X, K102Q, and K102X using primers listed in Table 1. The mutant sequences are shown in Supplementary Fig. 1.

The *Pdf* genomic DNA fragment (wild type or mutants) was inserted into a newly developed pUTK-attB vector at EcoR1 > BamH1 sites (Supplementary Fig. 8) for *attP* site-specific integration. To make *UAS-Pdf* constructs bearing wild-type or mutant *Pdf* coding sequences, full-length *Pdf* cDNA sequences were obtained from the corresponding genomic DNA clones by PCR using 5′-Pdf-R1/3′-Pdf-Xba primers (Table 1). The PCR products were inserted into the pUAST-attB vector at EcoR1 > Xba1 sites.

Generation of transgenic lines

All of the DNA constructs were integrated into the *attP40* site. DNA (215 ng/μL; Bischof *et al.* 2007) was injected into the embryos of *y w P{y[+t7.7]=nos-phiC31\int.NLS}; P{y[+t7.7]=CaryP}attP40* (BDSC #79604). Viable G0 male flies were crossed to balancer virgins (*y w; Bl/CyO, y*$^+$), and then, male transformants bearing the *mini-white* marker (G1) were selected to remove X-linked *nos-phiC31* integrase and then established as stocks. The introduced mutation sites were confirmed in their genomic DNAs by sequencing.

Antibodies and immunohistochemistry

Three different antibodies were generated in rats or rabbits (Genemed Synthesis). Rabbit anti-PDF was made against the entire PDF (NSELINSLLSLPKNMNDA-NH_2) and used at 1:3,000 dilution. Rat anti-cPAP was generated against 8 residues of the C-terminal end of the cPAP (LGPSVPIR) and used at 1:1,200 dilution. Rabbit anti-PAP was generated against 15 residues

Table 1. PCR primers used in this study.

Name	Sequence (5′ -> 3′)	Target region	Purpose
Pdf-Nsi-for	TGGTT GCCCA AATGC ATAGG CT	Pdf upstream up to Nsi site	To amplify Pdf gDNA
Pdf-BH-rev	CAGTG CGCAG GATCC ATGTT AACA	Pdf downstream up to BamH1 site	To amplify Pdf gDNA
K81Q-for	TGCCC ATCAG G**CAG**C GCAAC TCG	K81Q (AAG > CAG)	To remove cleavage site
K81-rev	CGGAT GGGCC CAAGG AGTTC TCA		
K81X-for	TGCCC ATCAG G**TAGT AA**CTC GGAGC TA	K81X (AAGCGC > TAGT)	To express cPAP only
G101X-for	ACATG AACGA TGCG**T AA**AAG *TAA*GC CCGGA	G101X (GGC > TAA)	To remove amidation site
G101X-rev	TCTTG GGCAG ACTCA ACAAG GAGTT G		
K102Q-for	ACGAT GCGGG C**CAG***T* AAGCC CGGA	K102Q (AAG > CAG)	To remove amidation site
K102-rev	TCATG TTCTT GGGCA GACTC AACA		
K102X-for	ACGAT GCGGG C**TAG***T* AAGCC CGGA	K102X (AAG > TAG)	To remove amidation site
3′-Pdf-Xba	cctgtctagatGTTGTACCAGATTTC	Pdf cDNA 3′end	To make UAS-Pdf (wt & mut)
5′-Pdf-RI	cgcgaattc ATTCG CAAGTC TCCTG CTGC	Pdf cDNA 5′end	To make UAS-Pdf (wt & mut)

Mutagenic nucleotides are indicated in bold face; endogenous termination codons (TAA) are in italics. Engineered restriction enzyme sites (EcoR1 and Xba1) or natural ones (Nsi1 and BamH1) are underlined.

located in the N-terminal region of the PAP domain (PDEERYVRKEYNRDL) and used at 1:1,200 dilution. Monoclonal anti-PDF-C7 obtained from Developmental Studies Hybridoma Bank was used at 1:100 (Cyran *et al.* 2005).

Immunohistochemical procedures were done as previously reported (Park *et al.* 2000). Briefly, dissected CNSs at around 8 h after light on were fixed in 4% paraformaldehyde overnight at 4°C, rinsed in 1× PBS (3 × 15 min each) and then in TNT (0.1 M Tris, PH 7.4; 0.3 M NaCl; 0.5% Triton X-100) (3 × 15 min each). The samples were then incubated in the blocking buffer (TNT containing 4% normal donkey serum) for 2 h at room temperature (RT). After incubation with primary antibodies at 4°C overnight, the samples were rinsed in TNT (6 × 15 min each) and then incubated with secondary antibodies conjugated with Alexa Fluor 594 or Alexa Fluor 488 (1:200 dilution; Jackson ImmunoResearch) for 2 h at RT. Fluorescent images were acquired by Olympus BX61 epifluorescence microscope. For the quantification, the immunosignals were acquired under the same exposure condition and the signal intensities were measured with ImageJ. Prism (ver. 9.4.1) was used to run the Student *t*-test or ANOVA followed by Tukey's multiple comparisons test and to generate graphs.

Analysis of the circadian locomotor activity rhythms

Circadian locomotor activities of adult males (3–5 d old) were monitored by an infrared emitter–detector system and recorded every 30 min using the Drosophila activity monitoring system (https://trikinetics.com/). Flies were entrained to 12-h light:12-h dark (12:12 LD) cycles for 4 d and then placed under constant darkness (DD) for additional 7–8 d. Chi-square periodogram analysis was performed with ClockLab software (Actimetrics), as described previously (Bahn *et al.* 2009). Flies that did not survive the entire assay period were excluded from the data analysis.

Results

Dibasic KR residues act as the cleavage site for proPDF

Studies with various neuropeptide precursors (pro-Neuropeptides) have suggested that monobasic or dibasic residues that are strategically positioned between the associated peptide and functionally active neuropeptide act as the proteolytic cleavage site (Veenstra 2000; Duckert *et al.* 2004; Hoshino and Lindberg 2012). The proPDF also contains dibasic KR residues in such a position; hence, cleavage at this site could be a key step, ultimately leading to the production of 2 final products, mPDF and cPAP (Fig. 1a. To ascertain if the KR residues serve as the cleavage site of proPDF, we generated 3 UAS constructs; a control *UAS-Pdf*^{WT} and mutant *UAS-Pdf*^{K81Q} and *UAS-Pdf*^{K81X} (Fig. 1b and Supplementary Fig. 1), each of which was inserted into the *attP40* site to eliminate any positional effects on the transgene expression (Markstein *et al.* 2008). K81Q substitution is intended to disrupt the cleavage event, thus producing a cleavage-defective proPDF form. K81X is to produce cPAP only by introducing a premature stop codon (represented by X).

To monitor ongoing proteolytic processing of the wild-type and mutant proPDF, we generated 3 antibodies: anti-cPAP for the detection of cPAP only and anti-PAP and anti-PDF to detect PAP and PDF regions, respectively, in both precursor and cleaved forms (Fig. 1a). To test if these antibodies detect PDFergic neurons specifically, the CNSs of wild-type flies were immunostained. The results show that each of the antibodies labeled all known PDFergic neurons in both larval CNS and adult protocerebrum (Supplementary Fig. 2). Next, we directed ectopic expression of both wild-type and mutant *Pdf* transgenes in the corazonin (Crz) expressing peptidergic neurons by using a *Crz-Gal4* to monitor the products from these constructs without any interference from endogenously expressed *Pdf*. Since a mature Crz neuropeptide is also derived from its larger precursor form (Supplementary Fig. 7), we expect that the corazonergic neurons contain all enzymes necessary for proPDF processing (Choi *et al.* 2005; Pauls *et al.* 2014). We focused primarily on the 8 pairs of ventral neurons (vCrz) located from the 2nd thoracic to 6th abdominal neuromeres because they are easily distinguishable from endogenous PDFergic neurons (Fig. 2j; Choi *et al.* 2005; Lee *et al.* 2008). All antibodies displayed strong immunostainings in the vCrz neurons expressing *Pdf*^{WT} (Fig. 2, a–c), and similar results were found in the brain Crz neurons (Supplementary Fig. 3). The data indicate that the wild-type proPDF was successfully produced and cleaved in the Crz neurons.

Expression of *Pdf*^{K81Q} was also detected with both anti-PDF and anti-PAP but not with anti-cPAP (Fig. 2, d–f), suggesting that the mutant proPDF remained uncleaved and that KR residues are indeed important for the cleavage. The lack of anti-cPAP signals is likely because the antigenic site for the anti-cPAP is sterically hidden in the absence of cleavage of proPDF. In support of this notion, all of the *Pdf*^{K81X}-expressing vCrz neurons were labeled well with both anti-cPAP and anti-PAP but none with anti-PDF (Fig. 2, g–i). These results raised the possibility that the exposed C-terminal residues of the cPAP might be important for the immunoreactivity with anti-cPAP. To test this, we made an additional construct (UAS-*Pdf*^{R80AX}) in which the C-terminal R residue of the cPAP is

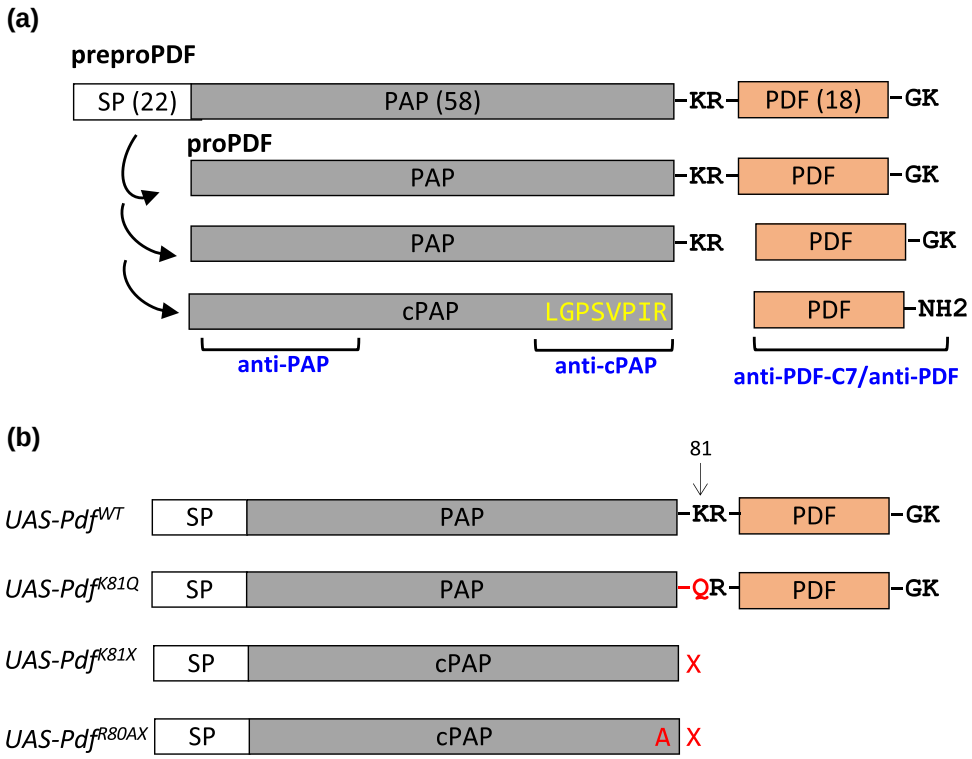

Fig. 1. Site-directed mutagenesis of the PC cleavage site of the proPDF. a) Schematics of the hypothetical maturation process of the PDF precursor. Numbers in parenthesis indicate amino acid residues in each domain deduced from the *Pdf* cDNA. Analysis with PrediSi (http://www.predisi.de/) and PSORT (https://www.genscript.com/tools/psort) predicted the first 22 aa to be a signal peptide. LGPSVPIR at the C-terminal of PAP is used as an antigenic site to generate anti-cPAP. Antigenic sites for the other 3 antibodies are also indicated (SP, signal peptide; PAP, PDF-associated peptide). b) *UAS-Pdf* constructs [wild-type (WT) and 3 indicated mutants] generated by site-directed mutagenesis (see also Supplementary Fig. 1).

replaced with Ala (Fig. 1b). Expression of this mutant form in the vCrz neurons was detected with anti-PAP but not with anti-cPAP (Fig. 2, k and l), confirming that the immunoreactivity of anti-cPAP requires the R residue exposed at the C-terminal end of the cPAP.

We also like to note that the expression of both cleavage-defective proPDF^{K81Q} form and cPAP only is detected in the somata as well as the axonal tracts of the vCrz neurons (Fig. 2 and Supplementary Fig. 3). These data suggest that the PAP domain is not only required but also sufficient for the trafficking of proPDF for the regulated secretory pathway (Gondré-Lewis *et al.* 2012). We propose that the proPDF is a preferred form for packaging into the secretory vesicles forming at the *trans*-Golgi network.

Overlapping localization of PDF and cPAP

Given the specificities of anti-cPAP and anti-PDF, we examined if there is any divergent subcellular distribution between PDF and cPAP in endogenous neurons. Both antibodies showed comparable immunosignals in the somata and neurites of all PDFergic neurons in the larval and adult CNSs (Fig. 3, a–d). Relatively weak cross-reactive signals of anti-PDF were noted in a few neurons near the dorsal projections of the LNs, a pair of neurons in the subesophageal area, and thoracic ventral neurons (Tv; Fig. 3, a and e). Simultaneous labeling with both antibodies revealed overlapping patterns from somata to axon terminals (Fig. 3, e–g), suggesting that the 2 final products, mPDF and cPAP, coexist in the secretory vesicles. Overlapping somatal signals of anti-cPAP and anti-PDF suggest that the cleavage of most proPDF, if not all, is completed before the vesicles enter the axonal tract. Noticeably stronger immunosignals near the axon terminals were consistently observed with both antibodies (Fig. 3, e–g), presumably reflecting the gradual accumulation of the secretory vesicles toward the terminals.

Rescue of *Pdf*^{01} mutant phenotype with *Pdf* transgenes

To see if both mutant forms (*Pdf*^{K81Q} and *Pdf*^{K81X}) are properly expressed and produced in the endogenous PDFergic neurons and capable of rescuing defective circadian locomotive activities of *Pdf*^{01} mutant flies (Renn *et al.* 1999), we made 3 genomic *Pdf* constructs, designated as *gPdf*^{WT}, *gPdf*^{K81Q}, and *gPdf*^{K81X} (Fig. 4a). Previously, we have shown that the 770-bp sequence upstream of the *Pdf* gene contains all *cis*-acting elements necessary for the spatiotemporal expression of *Pdf* (Park *et al.* 2000; Nair *et al.* 2020). A reason for making these lines, instead of utilizing the UAS/Gal4 system, is to imitate endogenous *Pdf* expression levels. Each genomic *Pdf* construct was inserted into the *attP40* site, and then, it was recombined genetically with the *Pdf*^{01} allele to eliminate endogenous *Pdf* products. As reported previously, the *Pdf*^{01}-encoded product (Y21X) is not immunoreactive with antibodies used here (Renn *et al.* 1999).

All tested antibodies displayed normal immunostaining patterns in the larval LNs and their dorsal projections in *gPdf*^{WT}; *Pdf*^{01} flies, verifying that the transgenically expressed proPDF^{WT} was properly produced and processed in the endogenous system (Fig. 4, bA–bC). Expression of *gPdf*^{K81Q} gave rise to products detectible with anti-PDF and anti-PAP (Fig. 4, bD and bF) but not with

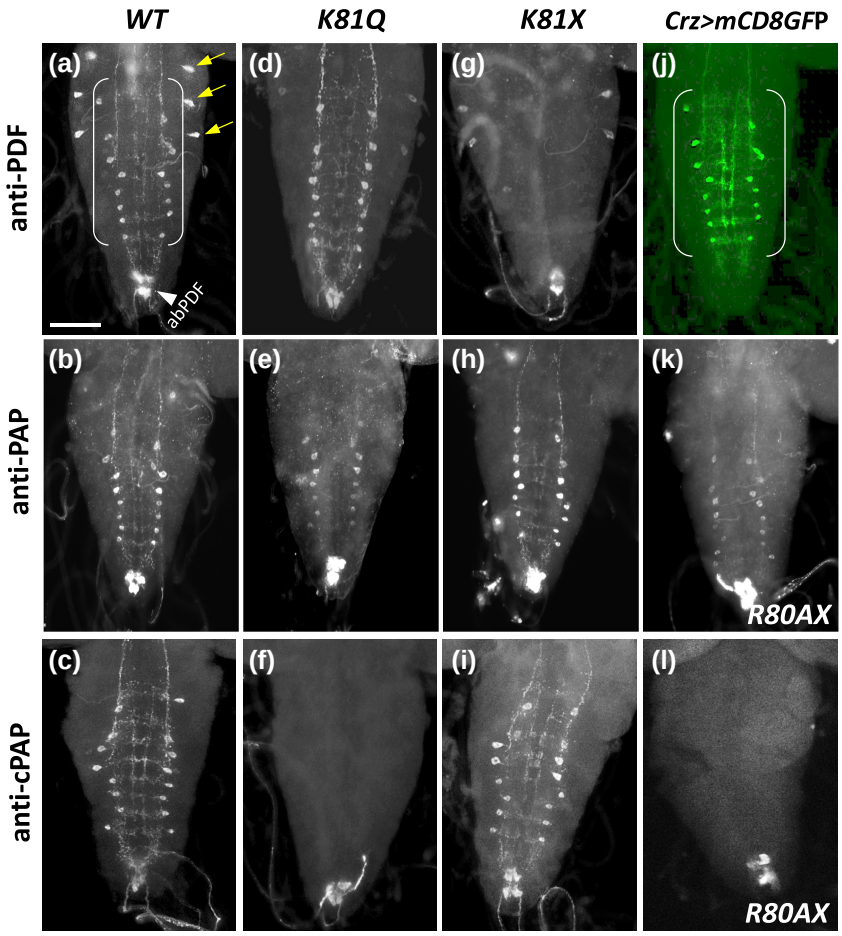

Fig. 2. Immunodetection of ectopically expressed mutant and wild-type *Pdf* in the vCrz neurons. At least 7 specimens were used for each antibody reaction. a–c) Expression of Pdf^{WT} (WT) was detected by all 3 antibodies. a) vCrz neurons are shown in the bracket. Arrows indicate nonspecific signals derived from anti-PDF. Endogenous PDFergic neurons located at the abdominal ganglia (abPDF) are indicated by an arrowhead. d–f) Expression of Pdf^{K81Q} (K81Q) was detected by anti-PDF d) and anti-PAP e), but not by anti-cPAP f). g–i) Expression of Pdf^{K81X} was not detected by anti-PDF g) but by both anti-PAP and anti-cPAP h, i). j) mCD8GFP-reported vCrz neurons in the bracket. k, l) Expression of Pdf^{R81AX} was detected by anti-PAP k) but not by anti-cPAP l). Scale bar, 100 μm.

anti-cPAP (Fig. 4bE), indicating that proPDF^{K81Q} also failed to be cleaved in the endogenous neurons, as shown in the vCrz neurons (Fig. 2f).

Since anti-PDF and anti-PAP are supposed to detect both proPDF^{K81Q} and wild-type forms equally, we expected comparable immunostaining levels between $gPdf^{K81Q}$ and $gPdf^{WT}$. However, we noticed significantly reduced anti-PDF immunoreactivities of this mutant form as compared to those of the wild-type one (Fig. 4, bA vs bD). Quantification analysis confirmed about 15% reduction of the immunosignals in the somata and about 58% reduction in the dorsal projections (Fig. 4, c and d). A similar reduction in immunosignal levels was also observed with anti-PAP (Fig. 4, bF vs bC). These results suggest that the uncleaved precursor is less stable in the LNs than is the wild-type one. Nevertheless, proPDF^{K81Q} seems to be delivered to the axon terminals; however, it is unknown if the uncleaved proPDF is exocytosed.

As expected, $gPdf^{K81X}$ expression was undetectable with anti-PDF (Fig. 4bG). To our intrigue, however, it also showed none or very weak immunoreactivities with anti-cPAP (Fig. 4bH) and with anti-PAP (Fig. 4bI). These data are in stark contrast to what we observed in the vCrz neurons in which the immunosignal levels were comparable between Pdf^{K81X} and Pdf^{WT} (Fig. 2, b and c vs h and i). A reasonable explanation is that cPAP alone is highly unstable and undergoes rapid degradation in the LNs but somehow remains stable in the Crz neurons. Since anti-cPAP signals are robust in $gPdf^{WT}$; Pdf^{01}, the coexistence of cPAP and mPDF following cleavage of proPDF seems to be necessary for the stability of cPAP at least in the LN neurons.

We further investigated if either the cleavage-defective mutant form or cPAP expression alone can restore the abnormal circadian phenotypes of Pdf^{01} (Renn *et al.* 1999; Bahn *et al.* 2009). During LD entrainment, control (w^{1118}) flies showed typical crepuscular activity patterns. Before light-off, the activities of w^{1118} increased steadily from ZT8, while slightly deviated patterns were shown by the WT and K102X rescued ones (Fig. 5), possibly due to different genetic backgrounds. In contrast, as reported previously (Renn *et al.* 1999), Pdf^{01} mutants displayed a broader evening peak produced by a sharper increase of activities, reaching the plateau at 1–1.5 h earlier than the control. Similar patterns were also observed in other transgenic lines (K81Q, K81X, G101X, and K102Q).

A majority of Pdf^{01} mutant flies were arrhythmic while a few of them were still rhythmic under constant darkness condition. Consistent with the immunosignals, $gPdf^{WT}$ transgene rescued the abnormal circadian phenotypes of Pdf^{01} mutants, whereas both $gPdf^{K81Q}$ and $gPdf^{K81X}$ failed to do so (Fig. 5 and Table 2).

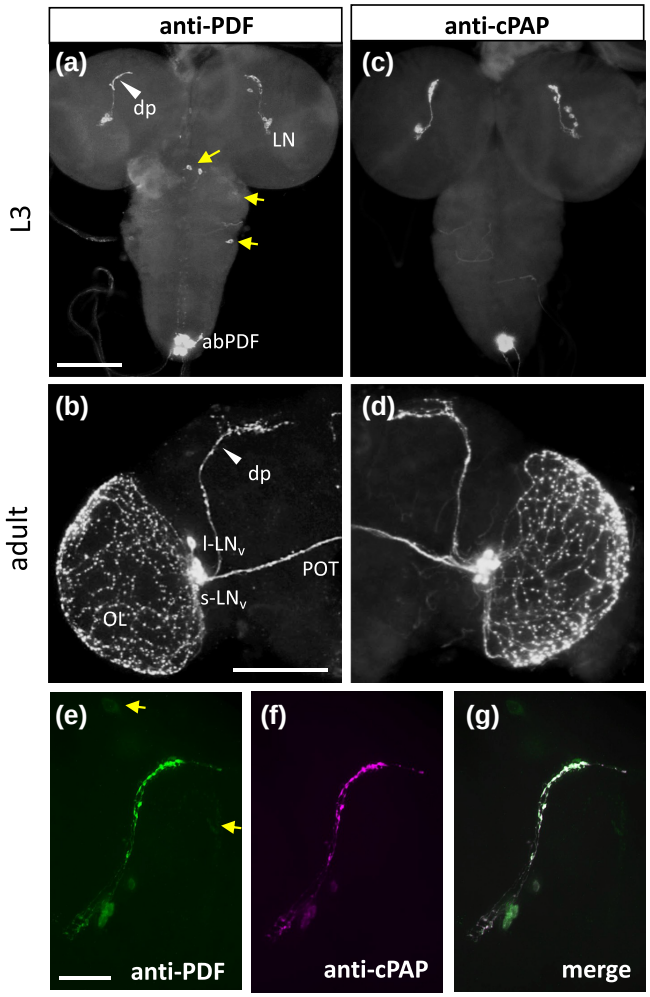

Fig. 3. Specificities of anti-cPAP and anti-PDF in the PDFergic neurons of wild-type larval and adult brains. a, c) Immunoreactivities with anti-PDF a) and anti-cPAP c) in the CNSs from wandering third-instar larvae ($n = 14$ for each). Arrows in a) indicate cross-reactive signals, which are absent in c). b, d) Immunoreactivities with anti-PDF b) and anti-cPAP d) in the adult brain ($n = 14$ for each). e–g) Simultaneous labeling with anti-PDF e), anti-cPAP f), and merger of the 2 g) in the larval brain lobe ($n = 28$). Cross-reactive signals of anti-PDF are indicated by arrows in e) (LN, lateral neurons; abPDF, abdominal ganglionic neurons; dp, dorsal projection of the LNs or s-LN$_v$s; OL, optic lobe; POT, posterior optic tract of the l-LN$_v$s). Scale bars, 100 μm (a), 50 μm b, e).

The lack of rescue by $gPdf^{K81Q}$ is unlikely due to lower PDF levels in the mutant. Having said this, PDF expression levels do not well correlate with the circadian phenotypes; even a single PDF neuron was able to drive robust circadian rhythms (Helfrich-Forster 1998). Nevertheless, the failure of $gPdf^{K81Q}$ in rescuing Pdf^{01} phenotypes supports that the proPDF per se is not a functional form and that the cleavage event at the KR site is indeed a cornerstone leading to the ultimate production of functional PDF.

Roles of C-terminal amidation for stability and function

The C-terminal amidation (a.k.a. α-amidation) has been suggested to be crucial for the stability and function of a variety of bioactive neuropeptides (Eipper *et al.* 1992). The amidation donor is C-terminally extended Gly (G), which is flanked typically with mono- or dibasic residues. The removal of these basic residues by a carboxypeptidase exposes the G residue, which is converted to an amide group by sequential enzymatic activities (Kolhekar *et al.* 1997; Pauls *et al.* 2014). Since proPDF also contains GK at the C-terminus of the PDF domain (Fig. 6a), the aforementioned reactions are likely to produce PDF-NH_2. However, whether the removal of C-terminal K and/or amidation is crucial for PDF's stability and function has not been assessed. To address this issue, we generated 3 transgenic lines, *UAS-*Pdf^{G101X}, *UAS-*Pdf^{K102Q}, and *UAS-*Pdf^{K102X}, as illustrated in Fig. 6a (see also Supplementary Fig. 1). G101X mutation removes both G and K residues, thus exposing Ala (A) at the C-terminus that is unmodifiable for amidation. In K102Q, the new C-terminal Q residue is not removed by the action of a carboxypeptidase, thereby hiding the G residue from amidating enzymes. The K102X mutant form ending with G residue possibly undergoes amidation reaction without the necessity of the K-removal step, which allows us to evaluate any role of the terminal basic residue(s) following G.

As done before, we first examined the expression of the mutant forms in the vCrz neurons. Both anti-PDF and anti-cPAP showed comparable levels of immunosignals between wild-type and amidation-defective G101X and K102Q forms (Fig. 6, bA–bC and bE–bG), suggesting that these mutants undergo normal proPDF cleavage and remain stable in the vCrz neurons. Second, by taking advantage of the amidation-defective forms, we tested PDF antibodies generated by us or others in the hope to find the one that can distinguish between amidated and non-amidated PDF. From our painstaking tests, we found that a mouse monoclonal anti-PDF-C7 raised against amidated PDF (Cyran *et al.* 2005) is specific to the amidated PDF. This antibody detected well PDFs from Pdf^{WT} expression that are expected to be amidated (Fig. 6bI) while it completely failed to recognize amidation-defective G101X and K102Q mutant forms (Fig. 6, bJ and bK). This antibody did not show any cross-reactivities in the wild-type larval and adult CNS (SupplementaryFig. 2D and Di). Together, these data demonstrate the specificity of anti-PDF-C7 to the amidated PDF. Remarkably, anti-PDF-C7 showed immunoreactivities in the vCrz neurons expressing Pdf^{K102X} (Fig. 6bL), suggesting that K102X could produce amidated PDF. However, it is notable that the anti-PDF-C7 signals were significantly weaker in the anterior 5 pairs of vCrz neurons as compared to the posterior 3 pairs (bracket in Fig. 6bL), implying nonuniformed capability of amidation reaction among vCrz neurons.

To address functional aspects of the amidation-defective mutant forms and the C-terminal basic residue(s) of PDF in the endogenous neurons, we created genomic mutant transgenes ($gPdf^{G101X}$, $gPdf^{K102Q}$, and $gPdf^{K102X}$) in Pdf^{01} background and then tested them with anti-PDF-C7. The results were quite consistent with what we observed in the vCrz neurons (Fig. 6, cA–cD). These data also suggest that bypassing the K-removal step (K102X) does not affect the subsequent amidation event; however, lower levels of immunosignals from K102X mutant (Fig. 6, cA vs cD) argue that the presence of K is somewhat important either for optimizing the amidation reaction or stabilizing precursor or intermediate forms or both.

In many *Drosophila* pro-Neuropeptides (proNPs), the functional neuropeptide domains are positioned internally in their precursors (e.g. Broek 2001; Park *et al.* 2003; Choi *et al.* 2005). In such cases, the amidation reaction must be preceded by a PC-mediated cleavage step (Supplementary Fig. 7). By comparison, the PDF domain is positioned at the C-terminus of the proPDF. Therefore, it might be unnecessary for the amidation and proPDF cleavage events to occur in an orderly manner. To

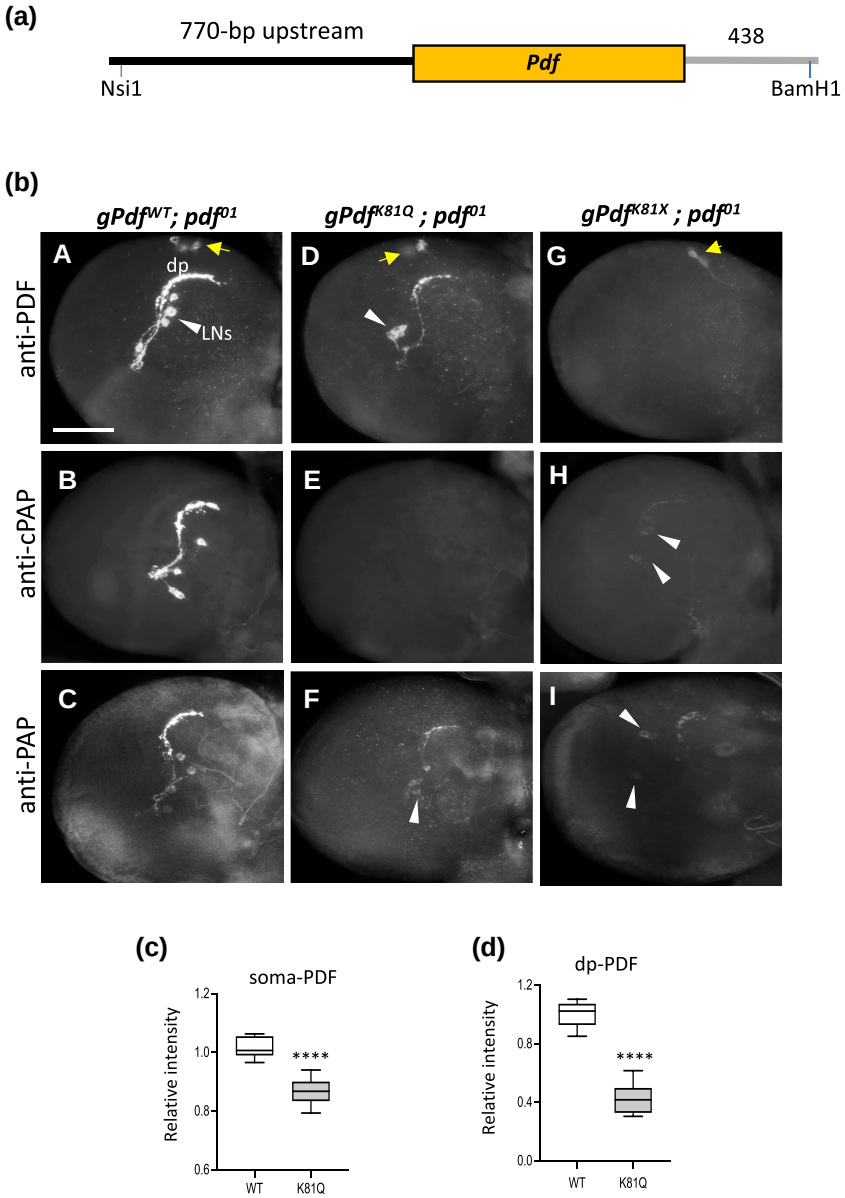

Fig. 4. Detection of $gPdf^{WT}$, $gPdf^{K81Q}$, and $gPdf^{K81X}$ expressed in the Pdf^{01} mutant background. a) A schematic diagram showing the genomic *Pdf* fragment, which includes 770-bp upstream and 438-bp downstream sequences of the *Pdf* gene. b) Immunohistochemical results with indicated antibodies and transgenes. Nonspecific anti-PDF immunoreactive signals are indicated by arrows in a), d), and g). Arrowheads point to somata of PDF-producing LNs. More than 10 larval brain samples were processed for each antibody reaction. Scale bar, 50 μm. c, d) Quantification of the signal intensities in LN-soma c) and dorsal projections d) for WT vs K81Q. (****$P < 0.0001$).

address this, we examined if the cleavage-defective proPDF^{K81Q} is amidated. We found robust immunoreactivities with anti-PDF-C7 in Pdf^{K81Q}-expressing vCrz neurons (Fig. 6bM). This antibody also showed immunoreactivities in the LNs of $gPdf^{K81Q}$; Pdf^{01} flies, but the signals were substantially weaker than in $gPdf^{WT}$; Pdf^{01} control (Fig. 6, cE vs cA). Since similar results were shown with anti-PDF (Fig. 4, bD vs bA), proPDF^{K81Q} seemed unstable in the LNs but not in the vCrz. Nevertheless, these data together indicate that the proPDF cleavage step is not a prerequisite for the C-terminal amidation.

To further assess if the amidation status affects the stability of PDF or proPDF in the LN neurons, we analyzed anti-PDF immunostaining in these transgenic flies. Both $gPdf^{G101X}$ and $gPdf^{K102Q}$ similarly showed slightly reduced immunosignals in the LN-somata but a pronounced reduction in the dorsal projections (Figs. 7, aA–aC, bA, and bB, for quantification). These results support the importance of amidation for the stability of proPDF and/or PDF. More severely reduced immunosignals in the nerve terminals might reflect the ongoing degradation of unamidated PDFs during transit along the axonal tracts.

Despite the subnormal stability of the amidation-defective mutant forms, PC-mediated processing of these mutant proPDFs is expected to occur normally, because the mutations are targeted to disrupt the C-terminal amidation events only. To our surprise, however, anti-cPAP signals were weaker in both mutants, although $gPdf^{K102Q}$ contained slightly more cPAPs than $gPdf^{G101X}$ did in both somata and dorsal projections (Figs. 7, aE–aG, bC, and bD, for quantification). These data can suggest that the lack

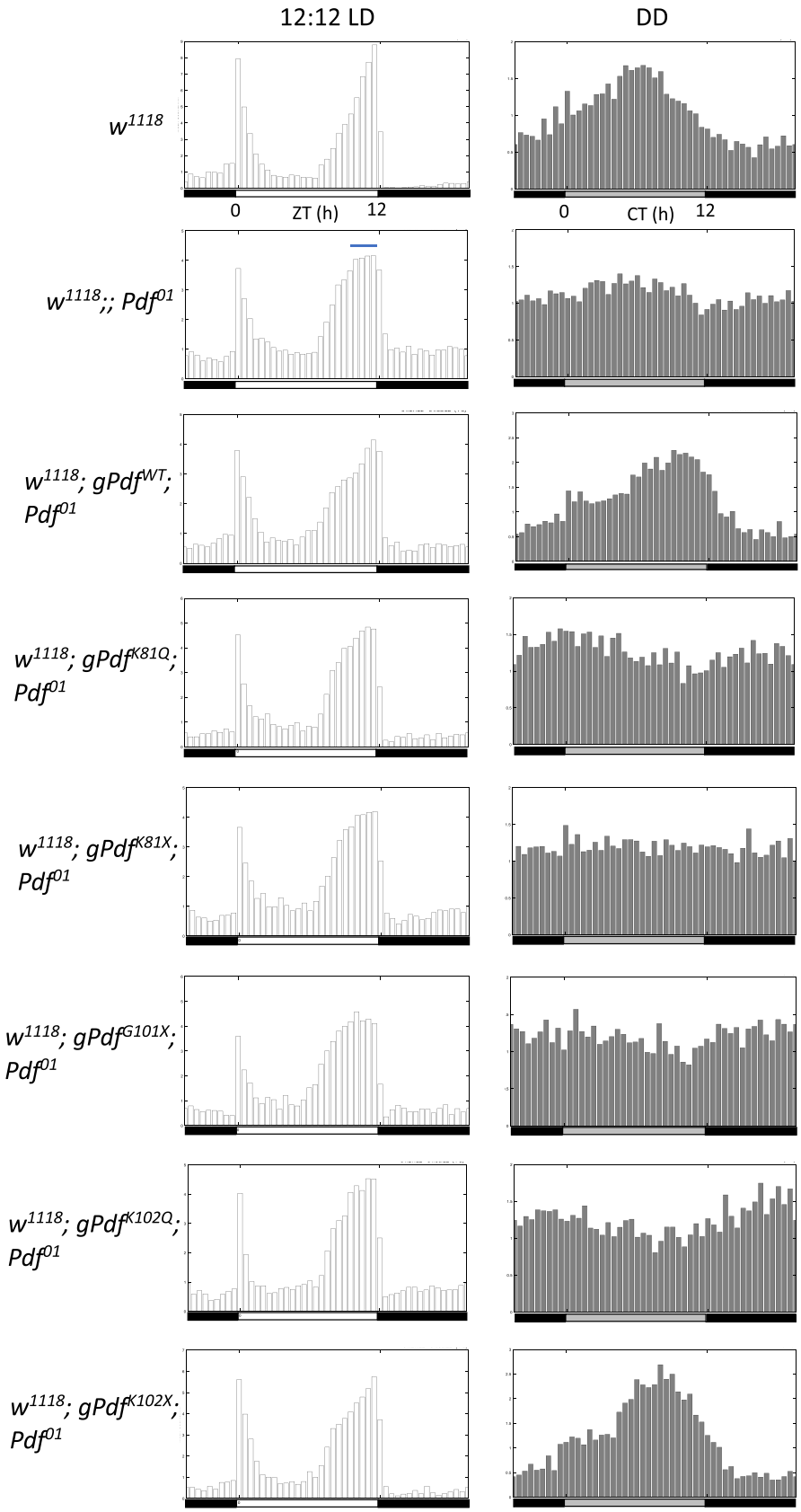

Fig. 5. Locomotor activity patterns of genetic control (w^{1118}) and various *Pdf* mutants in Pdf^{01} background. Average activity histograms indicate relative activity levels under 4 days of 12-h light:12-h dark conditions (LD, left), and 7 days of constant dark conditions (DD, right). Open, black, and gray horizontal bars under each histogram indicate light, dark, and subjective-light phase, respectively. A short horizontal line in the w^{1118}; Pdf^{01} indicates a broad evening activity peak that is a characteristic mutant behavior. (ZT, zeitgeber time; CT, circadian time; traditionally, ZT0 starts the light phase and ZT12 the dark phase).

Table 2. Circadian locomotor activity rhythms.

Genotype	*n*	AR	WR	*R*	Period (h) Mean ± SD	Power Mean ± SD
w^{1118}	22	0	1	21	23.4 ± 0.6	63.3 ± 36.5
w^{1118};; Pdf^{01}	30	15	6	9	22.5 ± 1.0	20.3 ± 24.9
w^{1118}; $gPdf^{WT}$; Pdf^{01}	30	3	2	25	24.2 ± 1.1	83.7 ± 47.7
w^{1118}; $gPdf^{K81Q}$; Pdf^{01}	30	12	6	12	23.2 ± 2.0	28.8 ± 32.5
w^{1118}; $gPdf^{K81X}$; Pdf^{01}	31	18	6	7	23.6 ± 2.7	14.2 ± 11.7
w^{1118}; $gPdf^{G101X}$; Pdf^{01}	31	14	8	9	23.9 ± 1.6	19.4 ± 20.0
w^{1118}; $gPdf^{K102Q}$; Pdf^{01}	32	16	9	7	23.4 ± 2.2	21.2 ± 28.4
w^{1118}; $gPdf^{K102X}$; Pdf^{01}	31	1	1	29	24.0 ± 0.9	78.8 ± 34.3
DvP-UmG; UAS-dcr2* × *UAS-amon RNAi*	36	9	14	13	24.9 ± 2.9	12.7 ± 9.7
*DvP-UmG** × *UAS-silver RNAi*	12	10	2	0	N/A	
*DvP-UmG** × *UAS-PHM RNAi*	9	6	0	3	22.8 ± 0.8	15.3 ± 3.0
*DvP-UmG** × *UAS-*Pdf^{WT}	14	1	1	12	23.8 ± 0.6	63.4 ± 50.7

Chi-square periodogram analysis with a confidence level at 0.025. *n*, number of flies tested; AR, arrhythmic (power < 1); WR, weakly rhythmic (1 ≤ power < 10); R, rhythmic ($P \geq 10$) under constant darkness. Both R and WR flies were counted for the period length. Power, an indicator of the strength of rhythmicity, was defined as the amplitude of peak above the significance line (Liu *et al.* 1991). Asterisks (*) indicate the DvPdf-Gal4, UAS-mCD8GFP double transgenic line.

of amidation somehow negatively influences the cleavage of proPDFs. Alternatively, the reduced anti-cPAP signals in the mutants might be due to decreased stability of cPAPs derived from the mutant precursors. Since the anti-PAP staining also showed significantly reduced signals in the mutants (Fig. 7c), it seems that lowered anti-cPAP signals (Fig. 7, aF and aG) are primarily due to the unstable nature of proPDF and/or cPAP derived from the C-terminal mutants.

Next, we analyzed the expression of $gPdf^{K102X}$ flies. First, anti-PDF signals were weaker in both somata and dorsal projections than the ones in $gPdf^{WT}$, but stronger than those in $gPdf^{G101X}$ and $gPdf^{K102Q}$ mutants (Fig. 7, aD, bA, and bB). Second, anti-cPAP signals were comparable to anti-PDF ones (Fig. 7, aH vs aD). We reason that the lower immunosignals are presumably due to the reduced stability of proPDF in the absence of C-terminal basic residue. We propose that the C-terminal basic residue acts as a protective measure to some extent against degradation and/or facilitates amidation reaction that also renders stability to final products.

We also wanted to see if amidation is essential for PDF's function in circadian behaviors. Both $gPdf^{G101X}$ and $gPdf^{K102Q}$ failed to rescue circadian phenotypes of Pdf^{01} mutant flies (Fig. 5 and Table 2). On the other hand, $gPdf^{K102X}$ fully rescued Pdf^{01}, verifying that the proPDF^{K102X}, despite slightly reduced expression, successfully produces functional PDF–amide, in which the amount is still sufficient for normal circadian behaviors. In this aspect, we remind that the cleavage-defective proPDF^{K81Q} was also amidated but unsuccessful to rescue the defective circadian behaviors of pdf^{01} flies, suggesting that the amidated proPDF per se is not functional.

Enzymes involved in the maturation of proPDF

Using the antibodies and RNAi tools, we assessed the roles of 3 different enzymes for the proPDF cleavage and amidation. The *Drosophila* genome contains *amontillado* (*amon*) encoding a single PC2 homolog (Siekhaus and Fuller 1999). *amon* is an essential gene as *amon*-null mutants are embryonic or early larval (L1–L2) lethal (Rayburn *et al.* 2003). Further genetic and peptidomics studies have shown that Amon is required for the cleavage of several proNPs to produce mature peptides, such as adipokinetic hormone (AKH) that is secreted from the neurohemal organs (Lee and Park 2004; Rhea *et al.* 2010; Wegener *et al.* 2011).

To find out Amon's role in cleaving proPDF, we knocked down *amon* in the PDFergic neurons. To avoid any possible negative effect on the endogenous *Pdf* expression, we employed a *DvPdf-Gal4* that drives strong reporter expression in the LNs (Fig. 8c; Bahn *et al.* 2009). We tested 4 different *amon*-knockdown (*amon*-KD) lines: UAS-*amon*-RNAi-78b (Rhea *et al.* 2010) and 3 UAS-*amon*-TRiP lines (GL01217, HMS02715, and HM05071). In response to the RNAi-78b expression, 30% of larval brain lobes lacked anti-cPAP signals (Fig. 8, a and b) and the remaining samples showed either very weak signals detected mainly in the dorsal projections or rather normal-looking ones. Two TRiP lines (GL01217 and HMS02715) showed reduced cPAP levels only in less than 10% of samples, while another TRiP line (HM05071) had no effect (Supplementary Fig. 4). Coexpressed mCD8GFP revealed intact LN neurons that were negative with anti-cPAP (Fig. 8d and Supplementary Fig. 4), indicating that *amon*-KD does not cause LN cell death or altered development.

Anti-PDF displayed significantly reduced signals in about 30% of *amon-RNAi-78b* samples but moderate-to-strong signals in the rest (Fig. 8, e vs f). Similar results were obtained with anti-PDF-C7 (Fig. 8, g vs h). None of the samples showed a complete lack of immunosignals, which is in contrast to the results from anti-cPAP. Taking these results together suggests that Amon is important for the proPDF cleavage and uncleaved precursors undergo the amidation process but their stability is compromised. These results are consistent with the reduced immunosignals of the cleavage-defective proPDF^{K81Q} in the LNs (Fig. 4bD). Low penetrance of the *amon*-KD is most likely due to the hypomorphic nature of RNAi lines. Having said this, ubiquitous expression of the *amon-RNAi* (78b) using *da-Gal4* or *tub-Gal4* showed that larvae developed normally and pupariated, and then, only about 6% of pupae (17 out of 287) became adults while the rest died during prepupal-to-pupal development. This sublethal phenotype of systemic *amon*-KD is much milder than *amon*-null mutants that show larval lethality before they reach the L3 stage (Rayburn *et al.* 2003).

The cleavage of proPDF by Amon yields 2 intermediate products, PAP-KR and PDF-GK. Subsequently, the C-terminal basic residues of both are expected to be removed by carboxypeptidase. Recently, *silver* (*svr*)-encoded carboxypeptidase D (CPD) was shown to be a key enzyme for this action in many *Drosophila* neuropeptides (Sidyelyeva *et al.* 2010; Pauls *et al.* 2019). To test Svr's role in the processing of both PAP-KR and PDF-GK, RNAi-mediated *svr*-KD was performed. *svr*-null mutant is early larval (L1) lethal (Sidyelyeva *et al.* 2006) and ubiquitous expression of *svr*-RNAi (*HMC02395*) phenocopied the lethal phenotype. All larval brains carrying *svr*-KD lacked immunosignals by anti-cPAP and anti-PDF-C7 (Fig. 9, a

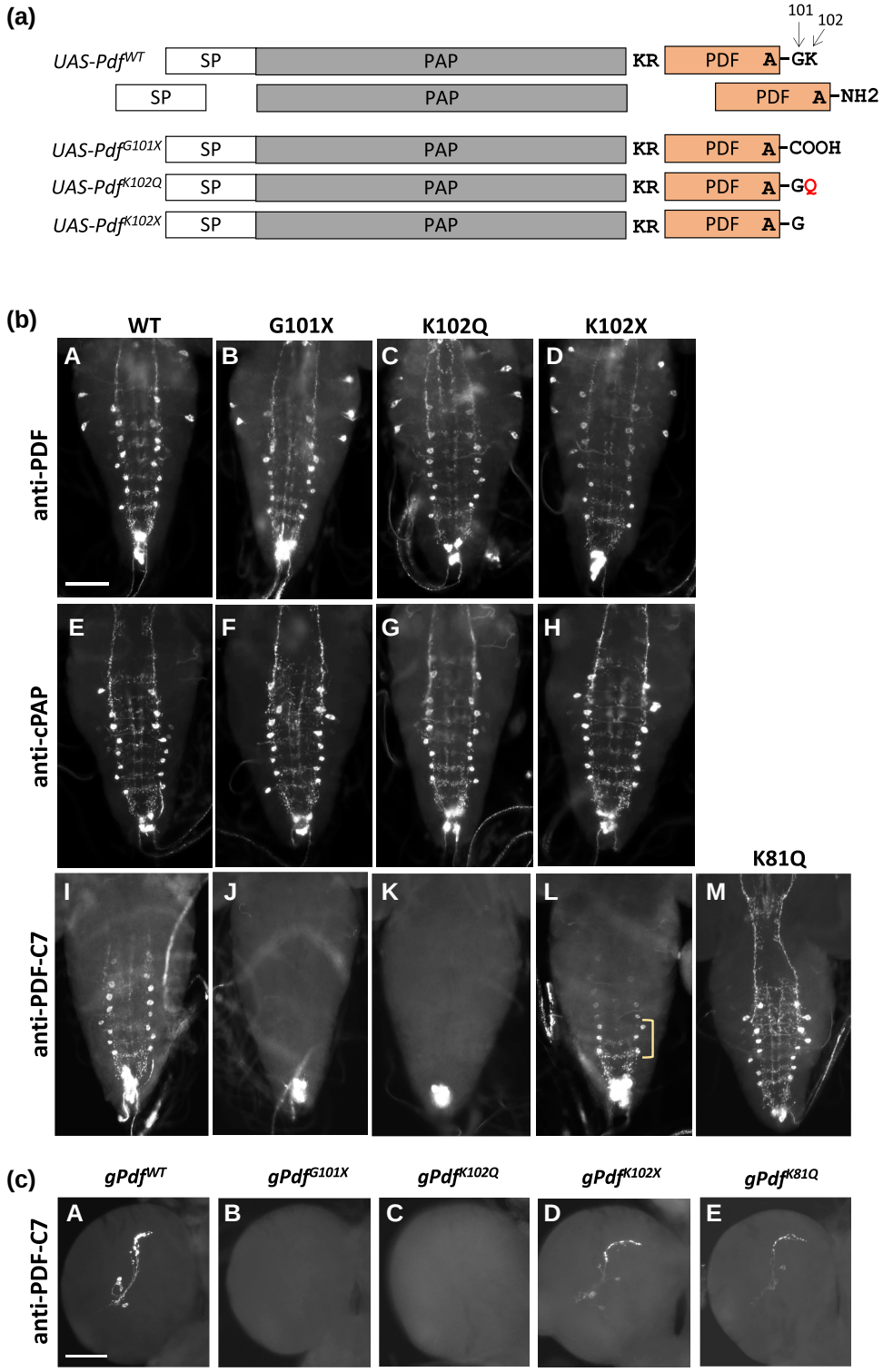

Fig. 6. Immunohistochemistry of the amidation-defective mutants. a) Schematics showing the *UAS-Pdf* constructs of WT and mutation sites at the C-terminal residues. b) Ectopic expression of indicated genotypes in the vCrz neurons (*Crz-Gal4* > *UAS-Pdf*) detected with respective antibodies ($n > 7$ for each panel). c) Larval PDFergic neurons expressing genomic versions of WT and mutant *Pdf* forms in the Pdf^{01} background. The neurons were stained with anti-PDF-C7. Representative images show LN neurons in a single larval brain hemisphere ($n > 14$ for each genotype). Scale bars, 100 μm (Ba), 50 μm (Ca). No immunoreactive signals were observed in G101X and K102Q mutants.

and c). Unexpectedly, both anti-PAP and anti-PDF also produced very weak signals that remained only in the somata (Fig. 9, b and d). *svr*-KD does not eliminate PDF neurons, as coexpressed mCD8GFP revealed normal PDF neurons (Fig. 9e). These data suggest that Svr's role is essential for the removal of the C-terminal basic residues from the PAP-KR and PDF-GK and that these intermediate forms are highly unstable and thus degraded quickly.

C-Terminal amidation requires sequential actions of PAL and PHM (Eipper *et al.* 1993). About 76% of *Drosophila* neuropeptides are confirmed or predicted to be amidated (Nassel and

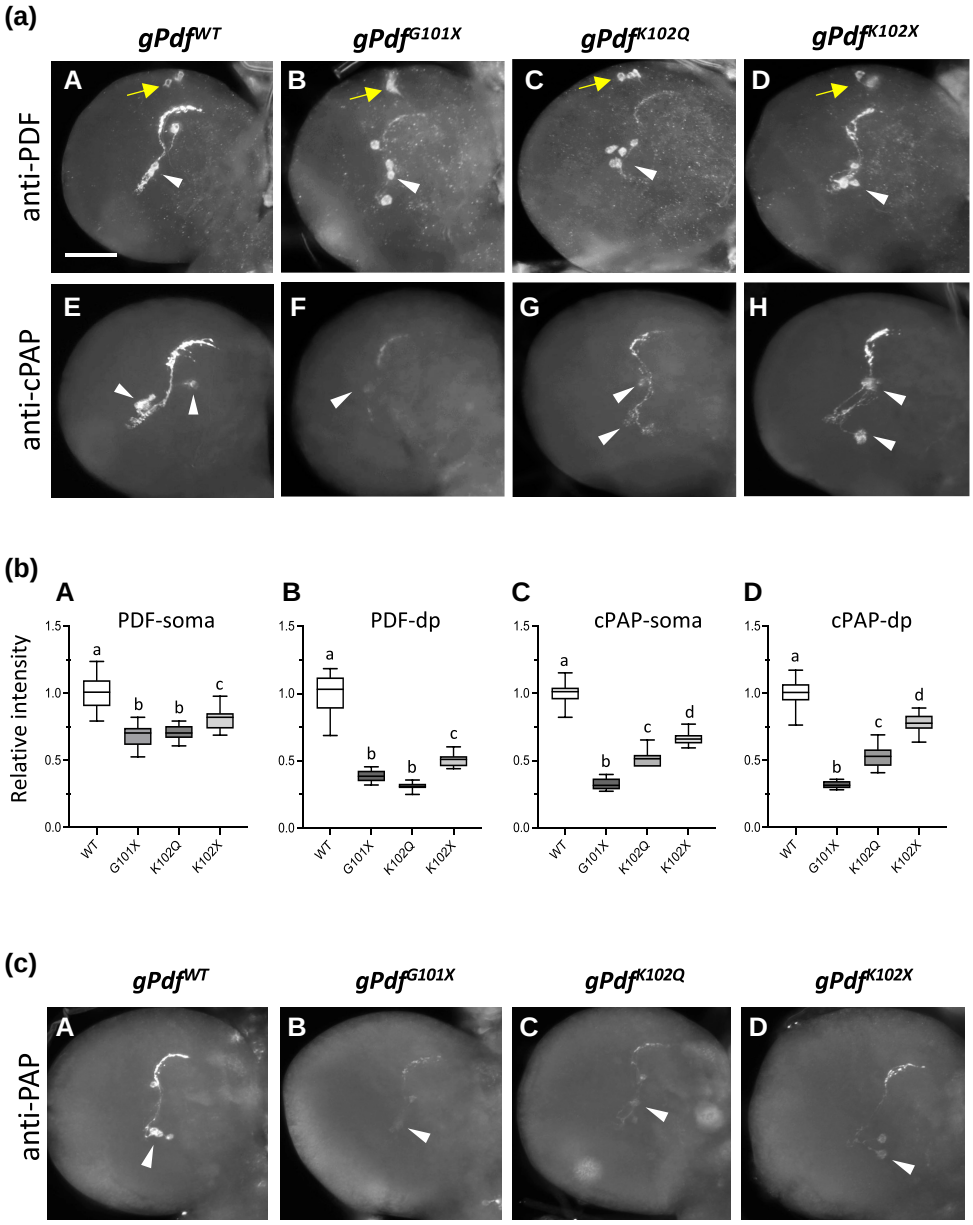

Fig. 7. Instability of C-terminal mutant PDF forms expressed in the LNs. Each genomic version of *Pdf* transgenes was recombined with the Pdf^{01} allele. aA–H) Expression of C-terminal mutant PDF forms was detected with indicated antibodies. Representative brain lobe images show LN neurons (arrowheads) and their dorsal projection ($n > 24$ brain lobes for each panel). Nonspecific signals of anti-PDF are indicated by arrows A–D). Scale bar in aA, 50 μm. bA–D) Quantification of signal intensities in somata and dorsal projection (dp). Different letters above the bars indicate statistical differences with a *P*-value less than at least 0.01. cA–D) Anti-PAP is used to detect the expression of WT and mutant forms. Arrows point to the LN somata.

Zandawala 2019). Our results support PDF amidation, but PHM's role in this is left unclear because of undetectable PHM immunoreactivities in the LNs (Taghert *et al.* 2001). Ubiquitous expression of *PHM-RNAi* (*HMC04080*) by *tub-Gal4* phenocopied late embryonic or L1 lethal phenotype of the *PHM*-null mutant (Jiang *et al.* 2000), proving effective *PHM*-KD by this line. *PHM*-KD in the PDF neurons eliminated anti-PDF-C7-immunosignals (Fig. 9f), verifying an essential role of PHM for PDF amidation. To check the amidation-defective PDF-G forms, we monitored *PHM*-KD brains with anti-PDF and found substantially weak immunosignals (Fig. 9g), indicating an unstable nature of PDF-G. These results further support that intermediate products are highly unstable and amidation provides neuropeptides with stability.

Next, we examined cPAP production in *PHM*-KD. Anti-cPAP immunosignals were absent in most samples (Fig. 9h) whereas anti-PAP showed weak but apparent immunosignals (Fig. 9i). Because anti-PAP detects both proPDFs and cPAPs, we speculate that the weak immunosignals are mostly attributed to proPDFs. These results indicate rapid degradation of cPAPs in the absence of amidated PDFs, which is consistent with the results from the expression of Pdf^{K81X} in the larval LNs (Fig. 4Bh). Based on all of these observations, we propose that upon completion of cleavage and amidation reactions, cPAP and amidated PDF remain closely associated with each other to protect them from degradation within the secretory vesicles.

We further tested if the knockdown of the PDF-processing enzymes phenocopies Pdf^{01} mutants. *amon*-KD flies showed only

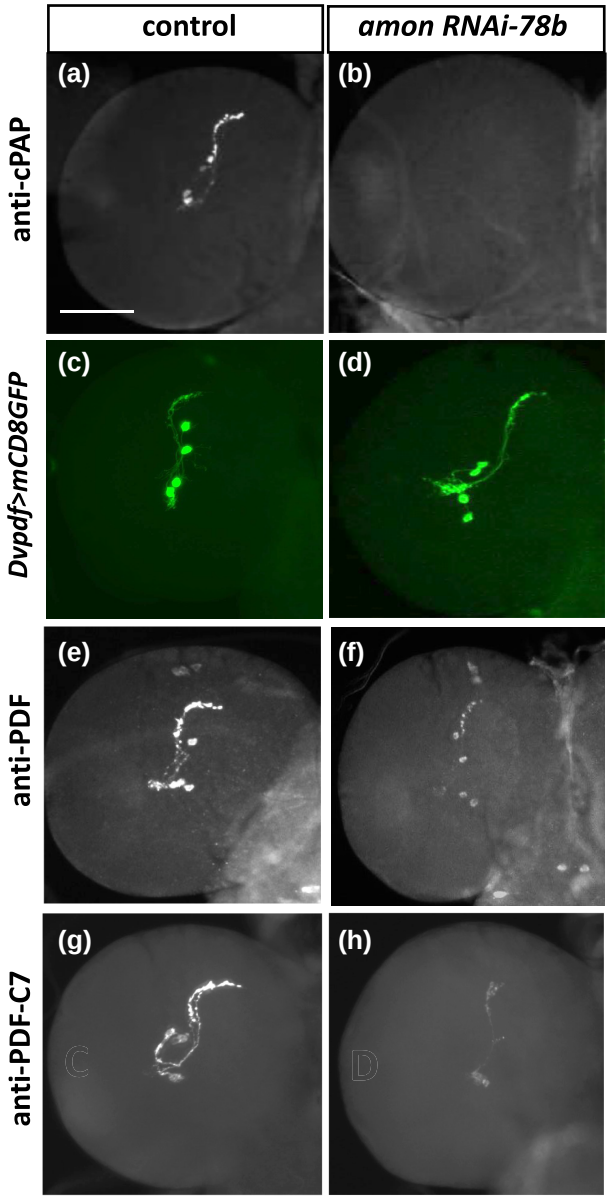

Fig. 8. Effect of *amon*-KD. The *UAS-mCD8GFP, DvPdf-Gal4* double transgenic line was crossed to w^{1118} (control, left column) or *UAS-amon-RNAi-78b* (right column) to knockdown *amon*. Larval PDFergic neurons were stained with anti-cPAP a, b), mCD8GFP c, d), anti-PDF (e, f), and anti-PDF-C7 g, h). At least 24 brains were processed for each antibody reaction. Scale bar, 50 μm a). The most severe cases of the *amon*-RNAi, which were observed in about 30% of samples, were presented here (see the text for a description of the variability). The results from additional *amon*-RNAi expression were also shown in Supplementary Fig. 4.

about 25% arrhythmicity, while a majority of the *svr*- and *PHM*-KD flies were arrhythmic (Table 2). The results are consistent with immunosignal ones.

Differential processing of proPDF between l-LN$_v$ and s-LN$_v$ neurons

Expression of Pdf^{K81Q} and Pdf^{K81X} showed stable presence in the vCrz neurons but did not so in LNs, suggesting that the stability of the mutant forms is differentially affected by cell types. There are 2 different clusters of PDFergic neurons in the adult brain, each containing 4 neurons: the s-LN$_v$s derived from persisting larval LNs and the other adult-specific l-LN$_v$s developed during metamorphosis. Although the somata of these 2 clusters are often adjacent to each other, they are unequivocally distinguishable by soma size, intensities of PDF immunosignals, and axonal projection patterns. In addition, *dimmed* (*dimm*), a key cell-fate determination factor for the peptidergic neurons, is expressed in the l-LN$_v$s but not in the s-LN$_v$s, indicating the differences of 2 clusters going beyond the morphology (Park *et al.* 2008). Given such differences, we wondered if the processing mechanisms of the proPDF are dissimilar between them. To explore this question, adult brains of $gPdf^{K81Q}$; pdf^{01} were monitored with anti-cPAP. As expected from the results in the larval LNs, the s-LN$_v$s were devoid of immunosignals (Fig. 10, b vs a). In contrast and to our surprise, the l-LN$_v$s contained fairly robust immunosignals in the somata and axonal projections in the optic lobe (Fig. 10b). These results clearly state differential cleavage mechanisms of proPDF operating between l-LN$_v$s and s-LN$_v$s. We propose that the s-LN$_v$s use mainly Amon-mediated cleavage at the consensus KR site but the l-LN$_v$s contain a yet unknown enzyme(s), perhaps in addition to Amon, that is capable of processing K81Q mutant to produce the cPAP.

We showed that the cPAP produced from $gPdf^{K81X}$ expression is highly unstable in the larval LNs (Fig. 4bH). We questioned if the stability of cPAP is also different between the 2 neuron clusters. Remarkably, anti-cPAP immunoreactivity showed to be largely normal in the l-LN$_v$s but little or none in the s-LN$_v$s of $gPdf^{K81X}$ flies (Fig. 10c). It appears that the presence of mPDFs is essential for cPAPs to maintain their stable existence in the s-LN$_v$s but dispensable for them in the l-LN$_v$s and vCrz neurons. Taking these results together suggests that the s-LN$_v$s are quite different from the l-LN$_v$s not only in the proPDF processing mechanism but also in the condition of the cPAP to maintain its stability. These results clearly state that the 2 LN$_v$ clusters are not identical in the biogenesis and maintenance of 2 final products of proPDF.

Cell-specific stability of PAP

It appears that the processing mechanisms of proPDF and susceptibility of cPAP to degradation in the absence of mPDF are diverse depending on the cell types. To test this idea further, we broadened Pdf^{K81Q} and Pdf^{K81X} expression to a larger population of larval neurons defined by *386Y-Gal4* which is inserted in the 3′ end of *amon*, thus largely reflecting endogenous *amon* expression patterns (Fig. 11aG; Taghert *et al.* 2001). The larval PDFergic LN neurons displayed weak but clear *386Y>nGFP* expression, indicating them as Amon positive (Supplementary Fig. 5A).

A fly line carrying *UAS-nGFP; 386Y-Gal4* was crossed to each of the UAS-*Pdf* transgene lines (UAS-Pdf^{WT}, UAS-Pdf^{K81Q}, and UAS-Pdf^{K81X}), and then, F1 larval CNS were processed with anti-PDF or anti-cPAP. Both antibodies produced similar patterns in *386Y>*Pdf^{WT}, suggesting that ectopically expressed proPDF^{WT} is properly processed in most, if not all, of Amon-positive neurons (Fig. 11, aA and aB). In the case of *386Y>*Pdf^{K81Q}, anti-PDF patterns looked comparable to those of *386Y>*Pdf^{WT}; however, only endogenous PDFergic neurons were detected with anti-cPAP (Fig. 11, aC and aD), indicating the lack of cleavage of the proPDF^{K81Q} mutant form in all Amon-positive larval neurons.

Compared to *386Y>*Pdf^{WT}, much fewer *386Y>*Pdf^{K81X}-expressing neurons were labeled with anti-cPAP (Fig. 11, aF vs aB). It indicates that the expressed cPAP remains stable in only a small population of Amon-positive neurons. To our intrigue, most of the cPAP-positive neurons appeared to be large peptidergic neurons; this prompted us to monitor the expression of Pdf^{K81X} in the peptidergic neurons using the *c929-Gal4* driver (a.k.a. *dimm-Gal4*; Hewes *et al.* 2003). While *386Y-Gal4* covers a large

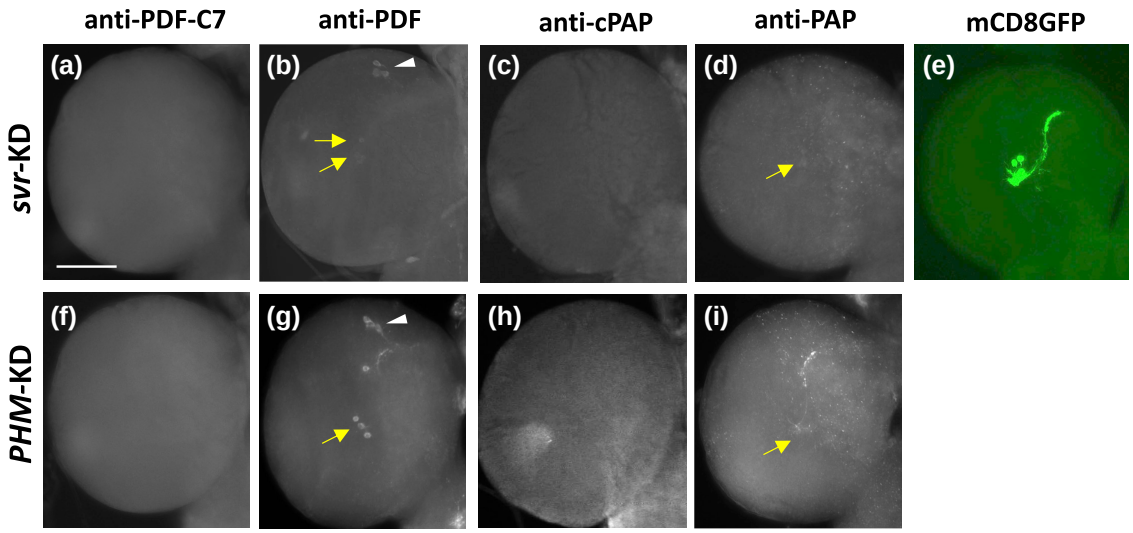

Fig. 9. Effect of *svr*-KD and *PHM*-KD on the *Pdf* expression. *DvPdf-Gal4* was crossed with RNAi lines of *svr* and *PHM*, and then, the offspring larval CNSs were stained with indicated antibodies. At least 24 brains were examined for each reaction. a–e) *svr*-KD. e) Coexpressed mCD8GFP shows intact PDF neurons. f–i) *PHM*-KD. Controls are the same as shown in Fig. 8. Arrows point to faintly stained LNs and arrowheads to nonspecific anti-PDF signals. Scale bar, 50 μm.

population of both peptidergic and nonpeptidergic neurons, *c929-Gal4* expression is limited to large-sized peptidergic neurons (Fig. 11bE). As such, *c929-Gal4* activity is absent in the small-sized larval LNs and their descendent adult s-LN$_v$s (Supplementary Fig. 5B; Park *et al.* 2008). The overall results recapitulate those from the *386Y-Gal4* driver. Both anti-PDF and anti-cPAP displayed similar patterns in the CNS of *c929>Pdf*^{WT} (Fig. 11, bA and bB), whereas anti-cPAP labeled much fewer neurons in *c929>Pdf*^{K81X} (Fig. 11, bD vs bB). Based on the positions and projection patterns, the large-sized peptidergic neurons positive for the cPAPs seem roughly equivalent to the ones shown in *386Y>Pdf*^{K81X} (Fig. 11, aF vs bD). We considered the possibility that the lack of cPAP immunoreactivities in some of the *c929>Pdf*^{K81X} neurons could be due to weak Gal4 activities in them. To test this, we examined the ectopic expression of *Pdf*^{K81X} with the 2 strong peptidergic drivers, *Akh-Gal4* and *ccap-Gal4* (Lee and Park 2004; Park *et al.* 2003). Null or very faint anti-cPAP signals were detected in both cases, implying that driver strength is not the main reason for the absence of detectable cPAP (Supplementary Fig. 6). Therefore, we conclude that only certain types of large-sized peptidergic neurons are capable of promoting the stability of cPAPs in the absence of mature PDF.

Discussion

Biosynthesis of the signaling peptide molecules requires precise intracellular sorting, trafficking, and processing of their precursors. Disruption of these steps would influence the production of bioactive peptides, which could be a cause of various human diseases (Hoshino and Lindberg 2012). Although the processing steps of proNPs have been investigated in both vertebrates and invertebrates (Fricker 2005; Hoshino and Lindberg 2012; Pauls *et al.* 2014), the molecular mechanisms underlying individual processing steps have not been fully understood. Combined studies utilizing powerful *D. melanogaster* transgenic tools with immunohistochemical and functional assays render this organism an ideal model for investigating the in vivo mechanisms of each processing step of proNPs in depth. Here, we took advantage of PDF as a case study, since its function in the regulation of the circadian behaviors and neuroanatomical features of PDF-expressing pacemaker neurons have been well established (Renn *et al.* 1999; Shafer and Yao 2014). In this study, we have investigated various mutations altering residues that are expected to be responsible for each processing event in both ectopic and endogenous conditions and RNAi-mediated knockdowns of individual genes that are known to encode neuropeptide-processing enzymes. The outcomes of these genetically manipulated proPDFs were measured by a combination of new and preexisting antibodies that monitor the products of processing events and by circadian behavior assays. As a result, we provide new insight into each processing step for the production of a functional PDF and the roles of the PAP/cPAP.

Roles played by PAP and cPAP

Bioactive neuropeptides or hormones are usually associated with larger prodomain in their precursors. The precursors, along with processing enzymes, are sorted at the trans-Golgi network (TGN) from which the secretory vesicles are formed, and then, matured vesicles follow the regulated secretory pathway (RSP; Tanaka 2003; Gondre-Lewis *et al.* 2012). The proPDF also consists of a relatively small PDF and a larger PAP domain. While the well-conserved PDF performs its function as a circadian modulator coupling several groups of clock gene-expressing neurons (Shafer *et al.* 2008; Im and Taghert 2010), the roles of the highly divergent PAP domain remain unexplored (Rao 2001; Matsushima *et al.* 2004; Bahn *et al.* 2009). A possible role of PAP is to make proPDF recognized and bound to the processing enzymes. In support of this, it has been shown that residues flanking the KR processing site are important, via the formation of a secondary structure, for the PC-mediated cleavage (Brakch *et al.* 1993) Structural analysis and comprehensive site-directed mutagenesis of this region would likely reveal the key residues in the PAP for binding proPDF to the processing enzymes.

Another possible role played by the PAP is the sorting/packaging of proPDF into a secretory vesicle. Expression of cPAP alone (*Pdf*^{K81X}) displays distribution patterns comparable to that of the wild type (*Pdf*^{WT}) in the somata and axonal projections of the vCrz neurons. Distribution patterns of a cleavage-defective proPDF^{K81Q} form are also similar to that of the wild type. These data strongly suggest that the PAP domain plays a critical role in sorting/packaging at TGN, and the precursor is a preferred form for loading into the vesicles budding from TGN. The processing

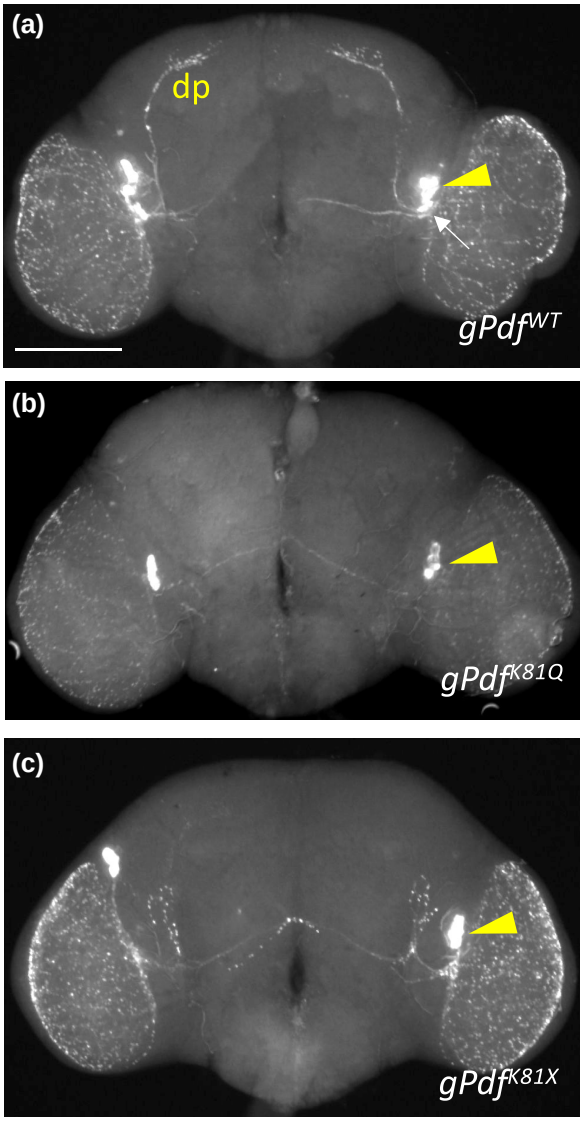

Fig. 10. Detection of cPAP in 2 adult-LN$_v$ neuronal clusters expressing a) $gPdf^{WT}$, b) $gPdf^{K81Q}$, and c) $gPdf^{K81X}$ in Pdf^{01} background ($n > 14$ brains for each genotype). l-LN$_v$s are indicated by arrowheads and s-LN$_v$s by an arrow a). s-LN$_v$s somata and their axons (dp) are undetectable in the mutants b, c). Scale bar, 50 μm.

enzymes are copackaged into the vesicles (Tanaka 2003; Gondre-Lewis *et al.* 2012), and our immunological data suggest that proPDF is rapidly processed shortly after the vesicles are formed from TGN. Sorting proPDF cargo into the budding vesicles at TGN might involve specific residues in the PAP. In line with this notion, studies with a human neuropeptide CART (cocaine- and amphetamine-regulated transcript) have shown that an obesity-causing missense mutation (L34F) in the prodomain caused mis-sorting of the precursors. As a result, the mutant pro-CARTs are poorly processed and then degraded, suggesting that the L34 residue is crucial for the trafficking of the pro-CART (Yanik *et al.* 2006).

Another role of the PAP suggested by our study is that it provides a protective mechanism of mPDFs from its degradation within the vesicles. Our data demonstrate that cPAPs derived from wild-type proPDF coexist stably with mPDFs, whereas expressed cPAPs alone are highly susceptible to degradation particularly in the pacemaker neurons, raising the possibility that cPAP and mPDF remain closely associated following the completion of processing steps. We reason that such an association can render stability to both parties by fending off the scrutiny of degrading enzymes enclosed in the secretory vesicles. In this regard, it is worth noting that a proteomics study with the dense core vesicles isolated from the secretory chromaffin cells identified various proteolytic enzymes in addition to PCs (Wegrzyn *et al.* 2010). The functions of these enzymes are seldom known yet but possibly involved in the quality control of secretory peptides within the vesicles.

Upon secretion from the axon terminals, the cPAP–mPDF complex might remain associated to avoid premature degradation of mPDF in the extracellular matrix. Such a protective mechanism could be essential for mPDFs to reach and activate the receptive neurons that are remotely localized (Shafer *et al.* 2008; Im and Taghert 2010). This idea is not outlandish. It is known that the precursor form of a paracrine TGF-beta ligand is processed intracellularly but its prodomain (called latency-associated peptide) and mature ligand remain noncovalently bound even in the extracellular matrix to protect the mature ligand (Derynck and Budi 2019). If so, does the secreted cPAP have its signaling function? This hypothesis is not favored, since the PAP region is poorly conserved in other insect species (Matsushima *et al.* 2004; Bahn *et al.* 2009). However, we cannot completely rule out a possible species-specific function of cPAP. Further experiments need to be done to determine if cPAP is truly exocytosed.

The biological significance of the C-terminal G and K residues

A majority of bioactive signaling peptides are modified with C-terminal amidation which is suggested to be important for their stability and receptor binding (Eipper *et al.* 1992). The consensus amidation signal is known to be "Gly-Basic-(Basic)," and removal of the basic residue(s) by a specific carboxypeptidase is essential to expose the amidation donor Gly. The PDF domain in the precursor contains "Gly-Lys (GK)" residues at the C-terminal end. Interestingly, the GK-type is more prevalent in dipteran insects, whereas GRK- or GRR-types are frequently found in orthopteran insects and crustacean species (Rao 2001; Matsushima *et al.* 2004; Bahn *et al.* 2009). Using amidation-defective mutant forms, PDF^{G101X} lacking GK and PDF^{K102Q} ending GQ, we demonstrated that the amidation is indeed essential for both stability and function of PDF.

Immunological characterizations of the PDF^{K102X} mutant form ending with G show that the C-terminal K residue is dispensable for PDF amidation. A few peptidyl venoms secreted from a scorpion that end with the C-terminal G are also amidated, supporting that the presence of C-terminal basic residue(s) is not a requirement for the amidation (Delgado-Prudencio *et al.* 2019). Then, is there any significant role played by the C-terminal basic residue(s)? We found $gPdf^{K102X}$ displaying significantly reduced immunoreactivities for PDF and cPAP, as compared to those of $gPdf^{WT}$ expression, indicating that K offers a certain level of protection to precursor and/or intermediates. The protection is rendered perhaps via interaction between the K-containing substrate and Svr carboxypeptidase since Svr–substrate interaction can secure the substrate from exposing it to the scrutiny of proteolytic enzymes. Alternatively, the basic residue removal step might facilitate optimal interaction between the substrates and amidating enzymes, thereby promoting the amidation reaction more effectively.

Lastly, we address whether 2 separate events, the C-terminal amidation and cleavage at the consensus KR site, are coordinated. In some proNPs including proCrz, the mature peptide domain positions internally; hence, the KR cleavage step must occur prior to

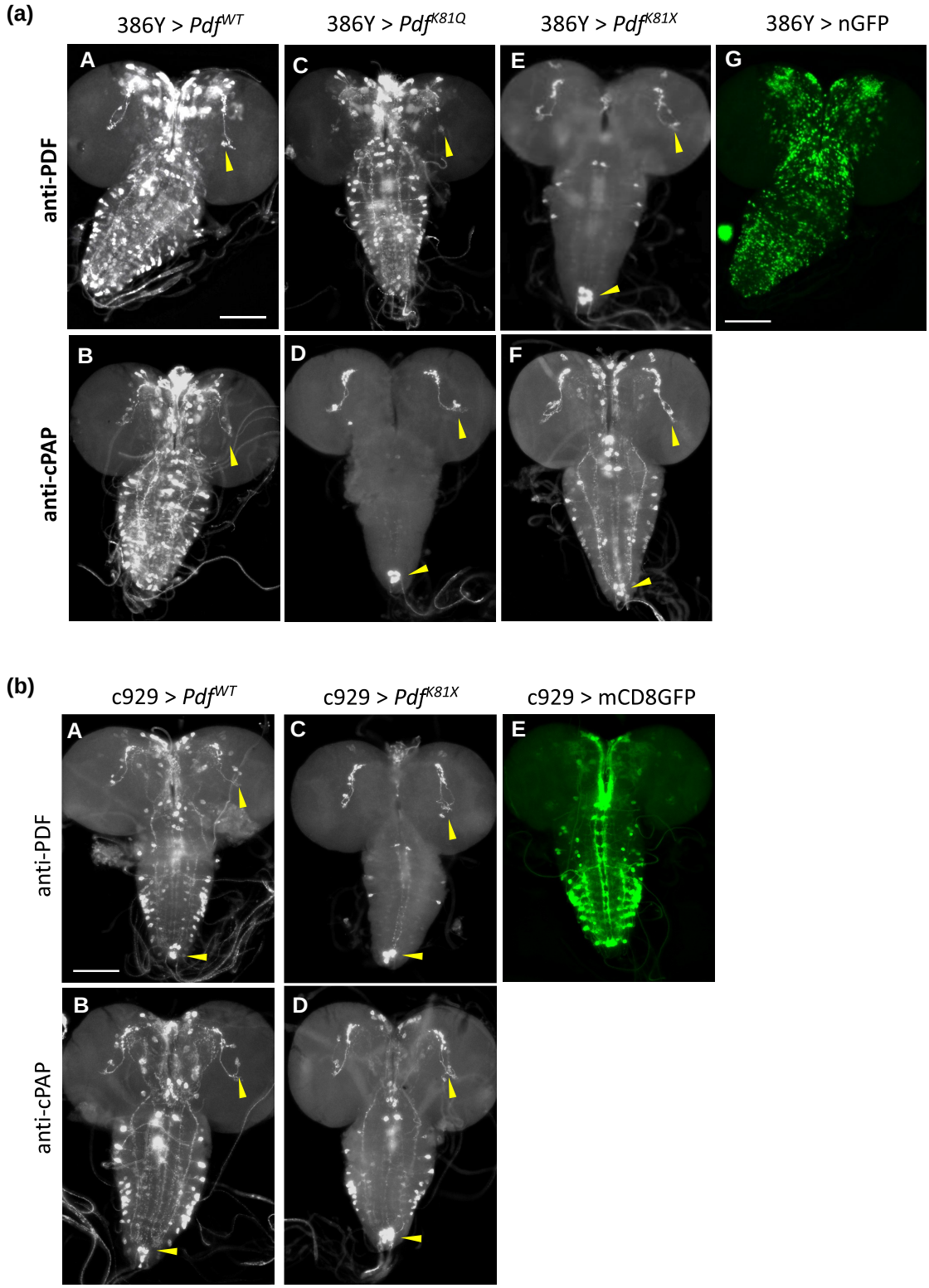

Fig. 11. Differential stability of cPAP-only expression in a) Amon-positive neurons or b) *dimmed*-positive peptidergic neurons. *UAS-nGFP, 386Y-Gal4* double transgenic line a) or *UAS-mCD8GFP; c929-Gal4* b) was crossed to indicated *UAS-Pdf* lines. At least 7 progeny CNSs were processed for each antibody reaction. Arrowheads indicate endogenous PDFergic neurons. aA, aB) Pdf^{WT} expression in ectopic sites is detected by both anti-PDF aA) and anti-cPAP aB). aC, aD) Ectopic Pdf^{K81Q} expression is detected with anti-PDF aC) but not with anti-cPAP aD). aE, aF) Ectopic Pdf^{K81X} expression is not detected with anti-PDF aE) but a few are positive with anti-cPAP aF). aG) 386Y-Gal4–driven nGFP expression pattern. Scale bar, 50 μm. bA, bB) Ectopic Pdf^{WT} expression detected by anti-PDF bA) and anti-cPAP bB). bC, bD) Ectopic Pdf^{K81X} expression sites are not detected with anti-PDF bC) and with anti-cPAP in fewer neurons as compared to WT bD). bE) *c929-Gal4*-driven *mCD8GFP* expression pattern. Scale bar, 50 μm.

amidation (Supplementary Fig. 7A). In contrast, since the PDF domain situates at the C-terminal of the precursor, the amidation of PDF is not necessary to follow the PC-mediated cleavage step (Supplementary Fig. 7B). Indeed, we demonstrated that the C-terminal events can occur independently of the KR processing step, as the cleavage-defective proPDF^{K81Q} is amidated. Conversely, amidation-defective mutant forms are all positive for cPAP production, a sign of the KR cleavage, indicating that the KR-processing event proceeds regardless of the amidation status. Therefore, an orderly manner of the 2 events is determined by the position of the neuropeptide domain within its precursor form.

Roles of enzymes involved in proPDF processing

We confirm in vivo roles of 3 key enzymes and the amino acid residues responsible for the processing steps of proPDF. Amontillado (Amon) acts to cut a proPDF at the consensus dibasic KR site, leaving 2 intermediate products, a PAP-KR and a PDF-GK. Silver (Svr) removes basic residues from both intermediates or proPDF, and then, PHM (peptidylglycine-α-hydroxylating monooxygenase) functions for the amidation of PDF. Both *Pdf* mutations and knocking down expression of enzymes cause moderate-to-severe degradation of unprocessed products, suggesting that the newly synthesized proPDF must be rapidly processed. This is supported by the overlapping patterns of anti-cPAP and anti-PDF signals in the somata and axonal projections of the PDFergic neurons. We propose that such a speedy processing is a key to optimizing PDF (and perhaps other neuropeptides) production and interruption of any of the processing steps can jeopardize the loss of intermediate products and the precursor. To accomplish this, it is conceivable that the processing enzymes form an exquisite complex or are arranged in a way to promote rapid interaction with substrates and perform multiple reactions effectively. Binding of proPDF and intermediate forms to the enzyme complex can also render a layer of protection from proteolytic degradation or harsh acidic milieu within the secretory vesicles. We propose that the secretory vesicles in the pacemaker neurons possess a quality-control system to monitor and remove any stalling or unfit intermediate products of PDF processing due to mutations or subnormal levels of processing enzymes.

Data availability

Fly strains and plasmids are available upon request. The authors affirm that all data necessary for confirming the conclusions of the article are present within the article, figures, and tables.

Supplemental material available at GENETICS online

Acknowledgements

We thank Hewes and Taghert for the *c929-Gal4* and *386Y-Gal4* lines and the Bloomington stock centers for various UAS-RNAi lines. We also appreciate the Lesaffre Corp. for their kind donation of yeast product for the fly food.

Funding

his work is supported by an NIH grant (R15-GM140423) to JHP and the National Research Foundation of Korea (NRF) grant (NRF-2020R1I1A3074467) to SY.

Conflicts of interest

The authors declare no conflict of interest.

Literature cited

Ahmad M, Li W, Top D. Integration of circadian clock information in the Drosophila circadian neuronal network. J Biol Rhythm. 2021; 36(3):203–220. doi:10.1177/0748730421993953.

Anstrom DM, Colip L, Moshofsky B, Hatcher E, Remington SJ. Systematic replacement of lysine with glutamine and alanine in *Escherichia coli* malate synthase G: effect on crystallization. Acta Crystallogr Sect F Struct Biol Cryst Commun. 2005;61(12): 1069–1074. doi:10.1107/S1744309105036559.

Bahn JH, Lee G, Park JH. Comparative analysis of Pdf-mediated circadian behaviors between *Drosophila melanogaster* and *D. virilis*. Genetics. 2009;181(3):965–975. doi:10.1534/genetics.108.099069.

Bischof J, Maeda RK, Hediger M, Karch F, Basler K. An optimized transgenesis system for *Drosophila* using germ-line-specific φC31 integrases. Proc Natl Acad Sci USA. 2007;104(9):3312–3317. doi: 10.1073/pnas.0611511104.

Blau J, Young MW. Cycling *vrille* expression is required for a functional *Drosophila* clock. Cell. 1999;99(6):661–671. doi:10.1016/S0092-8674(00)81554-8.

Brakch N, Boileau G, Simonetti M, Nault C, Joseph-Bravo P, Rholam M, Cohen P. Prosomatostatin processing in Neuro2A cells. Role of β-turn structure in the vicinity of the Arg-Lys cleavage site. Eur J Biochem. 1993;216(1):39–47. doi:10.1111/j.1432-1033.1993.tb18114.x.

Broeck JV. Neuropeptides and their precursors in the fruit fly, *Drosophila melanogaster*. Peptides. 2001;22(2):241–254. doi:10.1016/S0196-9781(00)00376-4.

Chen Y, Sun T, Bi Z, Ni JQ, Pastor-Pareja JC, Javid B. Premature termination codon readthrough in *Drosophila* varies in a developmental and tissue-specific manner. Sci Rep. 2020;10(1):8485. 10.1038/s41598-020-65348-8.

Choi C, Cao G, Tanenhaus AK, McCarthy EV, Jung M, Schleyer W, Shang Y, Rosbash M, Yin JCP, Nitabach MN. Autoreceptor control of peptide/neurotransmitter corelease from PDF neurons determines allocation of circadian activity in *Drosophila*. Cell Rep. 2012;2(2):332–344. doi:10.1016/j.celrep.2012.06.021.

Choi YJ, Lee G, Hall JC, Park JH. Comparative analysis of corazonin-encoding genes (Crz's) in Drosophila species and functional insights into Crz-expressing neurons. J Comp Neurol. 2005; 482(4):372–385. doi:10.1002/cne.20419.

Choi S-H, Lee G, Monahan P, Park JH. Spatial regulation of corazonin neuropeptide expression requires multiple cis-acting elements in *Drosophila melanogaster*. J Comp Neurol. 2008;507(2):1184–1195. doi:10.1002/cne.21594.

Choi Y-J, Lee G, Park JH. Programmed cell death mechanisms of identifiable peptidergic neurons in *Drosophila melanogaster*. Development. 2006;133(11):2233–2232. doi:10.1242/dev.02376.

Cyran SA, Yiannoulos G, Buchsbaum AM, Saez L, Young MW, Blau J. The double-time protein kinase regulates the subcellular localization of the *Drosophila* clock protein period. J Neurosci. 2005; 25(22):5430–5437. doi:10.1523/JNEUROSCI.0263-05.2005.

Delgado-Prudencio G, Possani LD, Becerril B, Ortiz E. The dual α-amidation system in scorpion venom glands. Toxins (Basel). 2019;11(7):425. doi:10.3390/toxins11070425.

Derynck R, Budi EH. Specificity, versatility, and control of TGF-β family signaling. Sci Signal. 2019;12(570):eaav518. doi:10.1126/scisignal.aav5183.

Duckert P, Brunak S, Blom N. Prediction of prohormone convertase cleavage site. Protein Eng Des Sel. 2004;17(1):107–112. doi:10.1093/protein/gzh013.

Eipper BA, Milgram SL, Husten EJ, Yun H-Y, Mains RE. Peptidylglycine α-amidating monooxygenase: a multifunctional protein with catalytic, processing, and routing domains. Protein Sci. 1993; 2(4):489–497. doi:10.1002/pro.5560020401.

Eipper BA, Stoffers DA, Mains RE. The biosynthesis of neuropeptides: peptide alpha-amidation. Annu Rev Neurosci. 1992;15(1):57–85. doi:10.1146/annurev.ne.15.030192.000421.

Fricker LD. Neuropeptide-processing enzymes: applications for drug discovery. AAPS J. 2005;7(2):E449–E455. doi:10.1208/aapsj070244.

Gondré-Lewis M, Park JJ, Loh YP. Cellular mechanisms for the biogenesis and transport of synaptic and dense-core vesicles. Int Rev Cell Mol Biol. 2012;299:27–115. doi:10.1016/B978-0-12-394310-1.00002-3.

Gunawardhana KL, Hardin PE. VRILLE controls PDF neuropeptide accumulation and arborization rhythms in small ventrolateral neurons to drive rhythmic behavior in *Drosophila*. Curr Biol. 2017; 27(22):3442–3453.e4. doi:10.1016/j.cub.2017.10.010.

Hardin PE, Panda S. Circadian timekeeping and output mechanisms in animals. Curr Opin Neurobiol. 2013;23(5):724–731. doi:10.1016/j.conb.2013.02.018.

Helfrich-Förster C. Robust circadian rhythmicity of *Drosophila melanogaster* requires the presence of lateral neurons: a brain-behavioral study of *disconnected* mutants. J Comp Physiol. 1998; 182(4):435–453. doi:10.1007/s003590050192.

Helfrich-Förster C. The neuroarchitecture of the circadian clock in the brain of *Drosophila melanogaster*. Microsc Res Tech. 2003; 62(2):94–102. doi:10.1002/jemt.10357.

Helfrich-Förster C. Neurobiology of fruit fly's Circadian clock. Genes Brains Behav. 2005;4(2):65–76. doi:10.1111/j.1601-183X.2004.00092.x.

Hewes RS, Park D, Gauthier SA, Schaefer AM, Taghert PH. The bHLH protein Dimmed controls neuroendocrine cell differentiation in *Drosophila*. Development. 2003;130(9):1771–1781. doi:10.1242/dev.00404.

Hoshino A, Lindberg I. Peptide biosynthesis: prohormone convertases 1/3 and 2. Colloq Ser Neuropeptides. 2012;1(1):1–112. doi:10.4199/C00050ED1V01Y201112NPE001.

Im SH, Taghert PH. PDF receptor expression reveals direct interactions between circadian oscillators in *Drosophila*. J Comp Neurol. 2010;518(11):1925–1945. doi:10.1002/cne.22311.

Jiang N, Kolhekar AS, Jacobs PS, Mains RE, Eipper BA, Taghert PH. PHM is required for normal developmental transitions and for biosynthesis of secretory peptides in *Drosophila*. Dev Biol. 2000; 226(1):118–136. doi:10.1006/dbio.2000.9832.

Jungreis I, Lin MF, Spokony R, Chan CS, Negre N, Victorsen A, White KP, Kellis M. Evidence of abundant stop codon readthrough in *Drosophila* and other metazoan. Genome Res. 2011;21(12): 2096–2113. doi:10.1101/gr.119974.110.

Kolhehar AS, Roberts MS, Jiang N, Eipper BA, Taghert PH. Neuropeptide amidation in Drosophila: separate genes encode two enzymes catalyzing amidation. J Neurosci. 1997;17(4): 1363–1376. doi:10.1523/JNEUROSCI.17-04-01363.1997.

Lee G, Kim KM, Kikuno K, Wang Z, Choi YJ, Park JH. Developmental regulation and functions of the expression of the neuropeptide corazonin in *Drosophila melanogaster*. Cell Tissue Res. 2008; 331(3):659–673. doi:10.1007/s00441-007-0549-5.

Lee G, Park JH. Hemolymph sugar homeostasis and starvation-induced hyperactivity affected by genetic manipulations of the adipokinetic hormone-encoding gene in *Drosophila melanogaster*. Genetics. 2004;167(1):311–323. doi:10.1534/genetics.167.1.311.

Liu X, Yu Q, Huang Z, Zwiebel L, Hall JC, Rosbash M. The strength and periodicity of *D. melanogaster* circadian rhythms are differentially affected by alterations in *period* gene expression. Neuron. 1991; 6(5):753–766. doi:10.1016/0896-6273(91)90172-V.

Markstein M, Pitsouli C, Villalta C, Celniker SE, Perrimon N. Exploiting position effects and the gypsy retrovirus insulator to engineer precisely expressed transgenes. Nat Genet. 2008;40(4): 476–483. doi:10.1038/ng.101.

Matsushima A, Sato S, Chuman Y, Takeda Y, Yokotani S, Nose T, Tominaga Y, Shimohigashi M, Shimohigashi Y. cDNA cloning of the housefly pigment-dispersing factor (PDF) precursor protein and its peptide comparison among the insect circadian neuropeptides. J Pept Sci. 2004;10(2):82–91. doi:10.1002/psc.511.

Mezan S, Feuz JD, Deplancke B, Kadener S. PDF signaling is an integral part of the *Drosophila* circadian molecular oscillator. Cell Rep. 2016;17(3):708–719. doi:10.1016/j.celrep.2016.09.048.

Nair S, Bahn JH, Lee G, Yoo S, Park JH. A homeobox transcription factor scarecrow (SCRO) negatively regulates Pdf neuropeptide expression through binding an identified cis-acting element in *Drosophila melanogaster*. Mol Neurobiol. 2020;57(4):2115–2130. doi:10.1007/s12035-020-01874-w.

Nässel DR, Zandawala M. Recent advances in neuropeptide signaling in *Drosophila*, from genes to physiology and behavior. Prog Neurobiol. 2019;179:101607. doi:10.1016/j.pneurobio.2019.02.003.

Ono D, Honma K, Honma S. Roles of neuropeptides, VIP and AVP, in the mammalian central circadian clock. Front Neurosci. 2021;15: 1–8. doi:10.3389/fnins.2021.650154.

Park JH. Downloading central clock information in Drosophila. Mol Neurobiol. 2002;26(2–3):217–233. doi:10.1385/MN:26:2-3:217.

Park JH, Hall JC. Isolation and chronobiological analysis of a neuropeptide pigment-dispersing factor gene in *Drosophila melanogaster*. J Biol Rhythms. 1998;13(3):219–228. doi:10.1177/074873098129000066.

Park JH, Helfrich-Förster C, Lui L, Rosbash M, Hall JC. Differential regulation of circadian pacemaker output by separate clock genes in *Drosophila*. Proc Natl Acad Sci USA. 2000;97(7): 3608–3613. doi:10.1073/pnas.97.7.3608.

Park JH, Schroeder AJ, Helfrich-Förster C, Jackson FR, Ewer J. Targeted ablation of CCAP neuropeptide-containing neurons of Drosophila causes specific defects in execution and circadian timing of ecdysis behavior. Development. 2003;130(12): 2645–2656. doi:10.1242/dev.00503.

Park D, Veenstra JA, Park JH, Taghert PH. Mapping peptidergic cells in *Drosophila*: where DIMM fits in. PLoS ONE. 2008;3(3):e1896. doi:10.1371/journal.pone.0001896.

Pauls D, Chen J, Reiher W, Vanselow JT, Schlosser A, Kahnt J, Wegener C. Peptidomics and processing of regulatory peptides in the fruit fly Drosophila. EuPA Open Proteom. 2014;3:114–127. doi:10.1016/j.euprot.2014.02.007.

Pauls D, Hararat Y, Trufasu L, Schendzielorz TM, Gramlich G, Kahnt J, Vanselow JT, Schlosser A, Wegener C. *Drosophila* carboxypeptidase D (SILVER) is a key enzyme in neuropeptide processing required to maintain locomotor activity levels and survival rate. Eur J Neurosci. 2019;50(9):3502–3519. doi:10.1111/ejn.14516.

Rao KR. Crustacean pigmentary effector hormones: chemistry and functions of RPCF, PDH, and related peptides. Amer Zool. 2001; 41:364–379. doi:10.1093/icb/41.3.364.

Rayburn LYM, Gooding HC, Choksi SP, Maloney D, Kidd AR, *et al.* *Amontillado*, the *Drosophila* homolog of the prohormone processing protease PC2, is required during embryogenesis and early larval development. Genetics. 2003;163(1):227–237. doi:10.1093/genetics/163.1.227.

Renn SCP, Park JH, Rosbash M, Hall JC, Taghert PH. A pdf neuropeptide gene mutation and ablation of PDF neurons each cause severe abnormalities of behavioral circadian rhythms in *Drosophila*. Cell. 1999;99(7):791–802. doi:10.1016/S0092-8674(00)81676-1.

Rhea JM, Wegener C, Bender M. The proprotein convertase encoded by amontillado (amon) is required in *Drosophila* corpora cardiaca endocrine cells producing the glucose regulatory hormone AKH. PLoS Genet. 2010;6(5):e1000967. doi:10.1371/journal.pgen.1000967.

Shafer OT, Kim DJ, Dunbar-Yaffe R, Nikolaev VO, Lohse MJ, Taghert PH. Widespread receptivity to neuropeptide PDF throughout the neuronal circadian clock network of *Drosophila* revealed by real-time cycle AMP imaging. Neuron. 2008;58(2):223–237. doi:10.1016/j.neuron.2008.02.018.

Shafer OT, Taghert PH. RNA-interference knockdown of Drosophila pigment dispersing factor in neuronal subsets: the anatomical basis of a neuropeptide's Circadian functions. PLoS ONE. 2009;4(12):e8298. doi:10.1371/journal.pone.0008298.

Shafer OT, Yao Z. Pigment-dispersing factor signaling and circadian rhythms in insect locomotor activity. Curr Opin Insect Sci. 2014;1:73–80. doi:10.1016/j.cois.2014.05.002.

Sidyelyeva G, Baker NE, Fricker LD. Characterization of the molecular basis of the *Drosophila* mutations in carboxypeptidase D: effect on enzyme activity and expression. J Biol Chem. 2006;281(19):13844–13852. doi:10.1074/jbc.M513499200.

Sidyelyeva G, Wegener C, Schoenfeld BP, Bell AJ, Baker NE, McBride SMJ, Fricker LD. Individual carboxypeptidase D domains have both redundant and unique functions in *Drosophila* development and behavior. Cell Mol Life Sci. 2010;67(17):2991–3004. doi:10.1007/s00018-010-0369-8.

Siekhaus DE, Fuller RS. A role for amontillado, the *Drosophila* homolog of the neuropeptide precursor processing protease PC2, in triggering hatching behavior. J Neurosci. 1999;19(16):6942–6954. doi:10.1523/JNEUROSCI.19-16-06942.1999.

Taghert PH, Hewes RS, Park JH, O'Brien MA, Han M, Peck ME. Multiple amidated neuropeptides are required for normal circadian locomotor rhythms in *Drosophila*. J Neurosci. 2001;21(17):6673–6686. doi:10.1523/JNEUROSCI.21-17-06673.2001.

Tanaka S. Comparative aspects of intracellular proteolytic processing of peptide hormone precursors: studies of Proopiomelanocortin processing. Zool Sci. 2003;20(10):1183–1198. doi:10.2108/zsj.20.1183.

Veenstra JA. Mono- and dibasic proteolytic cleavage sites in insect neuroendocrine peptide precursors. Arch Insect Biochem Physiol. 2000;43(2):49–63. doi:10.1002/(SICI)1520-6327(200002)43:2<49::AID-ARCH1>3.0.CO;2-M.

Vosko AM, Schroeder A, Loh DH, Caldwell CS. Vasoactive intestinal peptide and mammalian circadian system. Gen Comp Endocrinol. 2007;152(2–3):165–175. doi:10.1016/j.ygcen.2007.04.018.

Wegener C, Herbert H, Kahnt J, Bender M, Rhea JM. Deficiency of prohormone convertase dPC2 (AMONTILLADO) results in impaired production of bioactive neuropeptide hormones in *Drosophila*. J Neurochem. 2011;118(4):581–595. doi:10.1111/j.1471-4159.2010.07130.x.

Wegrzyn JL, Bark SJ, Funkelstein L, Mosier C, Yap A, Kazemi-Esfarjani P, La Spada A, Sigurdson C, O'Connor DT, Hook V. Proteomics of dense core secretory vesicles reveal distinct protein categories for secretion of neuroeffectors for cell–cell communication. J Proteome Res. 2010;9(10):5002–5024. doi:10.1021/pr1003104.

Welsh DK, Takahashi JS, Kay SA. Suprachiasmatic nucleus: cell autonomy and network properties. Annu Rev Physiol. 2010;72(1):551–577. doi:10.1146/annurev-physiol-021909-135919.

Yang Z, Sehgal A. Role of molecular oscillations in generating behavioral rhythms in *Drosophila*. Neuron. 2001;29(2):453–467. doi:10.1016/S0896-6273(01)00218-5.

Yanik T, Dominguez G, Kuhar MJ, Del Giudice EM, Loh YP. The Leu34Phe ProCART mutation leads to cocaine- and amphetamine-regulated transcript (CART) deficiency: a possible cause for obesity in humans. Endocrionol. 2006;147(1):39–43. doi:10.1210/en.2005-0812.

Editor: J. Simpson